CLIMATE FORCINGS AND THE NONLINEAR DYNAMICS OF GRASSLAND ECOSYSTEMS

BY

Matthew D Petrie

A thesis submitted to the faculty of the University of Kansas and department of Geography in partial fulfillment of the requirements for the degree of Master of Arts

Date	Nathaniel Brunsell, Chair
Date	
Date	
Date	

UNIVERSITY OF KANSAS

This thesis has been read by each member of the following graduate committee and is the approved Version of the following thesis.

Date	Nathaniel Brunsell Chair, Graduate Committee
Date	Member, Graduate Committee
Date	Member, Graduate Committee

ACKNOWLEDGMENTS

Thanks goes to Dave Mechem and Bryan Young for serving on the graduate committee; Jesse Nippert, for valuable information and data on Konza Prairie vegetation; Tyler Buck, for programming assistance; Nate Brunsell, for his patience, guidance, and good humor; and National Science Foundation EPSCoR 0553722 and KAN0061396/KAN006263 for funding this research.

Contents

Chapter 1

Abstract

The nonlinear interaction of climate forcings and ecosystem variables is instrumental in creating the temporal and spatial heterogeneity of grasslands. Ecosystem processes are a product of these interactions and vary in sensitivity to them across time. How forcings aggregate and shape ecosystem responses is an important aspect of grassland states and defines how they respond to changes in environmental conditions. Characterizing the relationship between climate drivers and ecosystem variables helps sharpen analysis of ecosystem flux dynamics during the growing season and identifies likely deviations from mean functioning.

To address the question of how climate forcings and ecosystem variables interact to shape seasonal water and carbon dynamics in grasslands, this thesis is split into two analysis chapters. The first (Chapter 3) is a characterization of water and carbon flux responses to variable precipitation timing and magnitude. Particular focus is placed on temporal sensitivity to inputs, seasonality in water flux dynamics, and the linkage between precipitation, soil moisture, evapotranspiration, and potential evaporation. Chapter 4 extends International Panel on Climate Change (IPCC A1B) regional climate scenario projections for the Central Plains of the United States to

assess mesic grassland responses. The specific focus is assessing the ecosystem response to increased precipitation variability, increased potential evaporation, and earlier growing season onset. Effects of these forcings are shaped by simulations of constant and seasonally-varying water-use efficiency to assess the role of vegetation on grassland carbon assimilation, and also to explore species-specific responses at the Konza Prairie in North Central Kansas, USA. Results from both chapters show variation in seasonal sensitivity of fluxes to precipitation, with varying relationships between drivers, variable conditions, and fluxes. This research provides for a better understanding of ecosystem processes and provides assessment of the magnitude and extent that forcing variation has on grassland function. Results from the second chapter show increased seasonal water and carbon flux variability and increased frequency of water stress conditions. Vegetation responses suggest climate change will impact species and habitat compositions through changing environmental conditions and partitioning of carbon assimilation periods. This illustrates potential effects to grassland functioning and growing season dynamics.

Chapter 2

Introduction

Mesic grasslands exhibit specific ecologic and hydrologic responses to climatic conditions. Local climate and related environmental conditions ($\leq$ 100 m^2) are largely responsible for grassland functional ecology and economic uses. Relationships between climate, ecology, and hydrology are, in fact, interactions; grasslands are shaped by and provide feedback to dominant combinations of forcings and local dynamics. Local interactions, therefore, are largely-responsible for grassland ecology and economic uses. Mesic grassland vegetation, for example, is limited by seasonal soil moisture availability, a product of precipitation, potential evaporation, and biotic interaction (Rosenberg et al., 1999). The ecology and economy of these grasslands is valuable; the Central Plains of the United States are the center of grain and livestock productivity in North America and also encompass numerous grassland types and support diverse species assemblages (Knapp et al., 1998). Grasslands are among the most-threatened of biomes; land-use change has reduced the tallgrass prairie of North America to a fraction of its former range (Knapp et al., 1998); this shift may alter regional carbon balances and response to climate (Ham and Knapp, 1998). Climate change may also affect agriculture and rangeland uses as soil moisture dynamics are

altered (Brunsell et al., 2010; Rosenberg et al., 1999). The way climate and ecology interact to shape grassland functioning dictates how the ecologic functioning and economic vitality of these ecosystems are affected by changing climate.

The ecology and hydrology of grassland ecosystems are shaped by the temporal interactions of climate forcings and ecosystem variables such as precipitation, evaporation, and photosynthesis. While the basic relation of these is understood, it is difficult to apply their in-situ interaction at larger scales. The cause of this is complex, nonlinear interaction between drivers and variables across space and time. Ecosystem variables and fluxes are the product of continual evolution of driver and variable interactions across time; understanding how these relationships exist and change is fundamental for understanding how grasslands work.

Accurate characterization of major processes is a useful way to assess the complex mechanics of ecosystem functioning. The value in this is accurate representation of nonlinear driver and variable relationships independent of extensive local data and difficult scale representation. Low-dimensional modeling and statistical representation offer frameworks for this focus (Guswa et al., 2002; Makela et al., 1996). They can be used in accurate representation and assessment of earth system processes, including seasonal water balance dynamics (Daly and Porporato, 2005), spatial and temporal vegetation (Porporato et al., 2003), and shifts in vegetation optimality and carbon assimilation (Caylor and Rodriguez-Iturbe, 2003; Vico and Porporato, 2008). Accurate relationship characterization and low-dimensional application have wide theoretical and applied value as well; these include thermodynamic optimality applications (Kleidon and Schymanski, 2008), energy balance partitioning and scale representation (Brunsell et al., 2010), and hydrology (Porporato et al., 2003, 2004).

This thesis focuses on two components of nonlinear ecosystem dynamics and grassland functioning. The first is a low-dimensional characterization of precipitation vari-

ability on growing season water and carbon dynamics across the Kansas River Basin precipitation gradient. The second component extends this to focus on carbon fluxes and likely vegetation responses to climate change. Understanding response characteristics is important for evaluating how ecosystem conditions relate to seasonal sensitivity to drivers and for predicting the effects of climate change in mesic grasslands. This chapter determines the major relationships and timescales involved in ecologic and hydrologic functioning and explores likely states and deviations of fluxes during the growing season.

To explore the question of how climate forcings and ecosystem variables interact to shape seasonal water and carbon dynamics in grasslands, this thesis characterizes the variable relationships governing flux seasonality and the likely ecosystem responses. General goals, organized from Chapters 3 and 4, are to: 1) characterize precipitation variability, through timing and magnitude deviation, as an ecological driver in the Kansas River Basin; 2) explore the seasonal dynamics of water and carbon fluxes in grassland ecosystems; 3) assess how vegetation and climate forcings shape growing season vegetation carbon assimilation; and 4) identify potential responses of vegetation carbon assimilation in the Konza Prairie, Kansas, USA, to altered climate forcings. These goals provide a more-complete understanding of the nonlinear, driving relationships that govern mesic grassland functioning during the growing season. Understanding the effects of changing climate in the Kansas River Basin and Konza Prairie is critical for effective resource management and planning, and is also applicable to the ecology and hydrology of semiarid systems; many are shaped by similar climate forcings.

Chapter 3

Precipitation variability and the ecohydrology of grasslands

3.1 Introduction

Ecohydrologic interactions are of considerable importance to ecosystem functioning and are often related to local characteristics such as vegetation type and dispersion, soil composition, and water availability. Interplay between climate, soil moisture, and vegetation is of particular interest since these largely determine landscape patterns and are often used to quantify ecologic function (Rodriguez-Iturbe et al., 2001). Soil moisture is identified as the primary linkage between climate, ecology, and atmospheric responses and feedbacks (Guswa et al., 2002; Rodriguez-Iturbe et al., 2001; Teuling et al., 2006,b).

The nonlinearities inherent to interactions within water, energy, and carbon cycles are an important and confounding characteristic of ecosystems. The basic individual and collective functions of these mass and energy fluxes are understood, but their spatial and temporal interactions are more complex, especially where ecosys-

tem fluxes have varying support between spatial scales, and between instantaneous, daily, seasonal, and annual timescales. Ecosystem function is a complex product of biotic coevolution and feedbacks between the environment and the biosphere where flux-dynamics are a product of continual interaction between state processes at different spatial and temporal scales. Understanding how relationships between ecosystem drivers, processes, and fluxes exist and change across space and time is a key component to understanding how ecosystems work.

Significant groundwork is available for understanding feedback relationships across water and carbon cycles (Raupach, 1995) but less is known about the interdependence and nonlinearity of these to energy and mass fluxes within specific locations (Brunsell and Gillies, 2003; Brunsell, 2006). The elasticity of mean fluxes produces heterogeneity in mass and energy fluxes as they are impacted by feedbacks with other variables operating at different spatial and temporal scales (Brunsell and Gillies, 2003). Understanding how this translates to ecohydrology is important as parameterizations may be implemented at non-representative scales if the dynamics of their individual and collective roles are not determined (Brunsell and Gillies, 2003). Scale misrepresentation limits the characterization of landscape features and ecohydrologic relationships and can subjugate understanding to arbitrary spatial focus (Alessandri and Navarra, 2008; Brunsell, 2006; Guswa et al., 2002; Kalma et al., 2008). Large and small-scale analysis both provide valuable insight on ecosystem functioning but are limited as a snapshot within their spatial and temporal support. Instead, it may be valuable to first understand the roles of forcing mechanisms as they interact across spatial and temporal scales to create states and deviations within and across ecosystems (Brunsell and Young, 2008).

Problems associated with understanding ecosystem nonlinearities have promoted analysis techniques that attempt to account for a large amount of ecosystem complex-

ity (Sridhar et al., 2002), those that conduct top-down and bottom-up parameterizations (Jacobs et al., 2003; Stephenson, 1998), and those that focus on major relationships between inputs and responses (Jarvis, 1976; Koster and Suarez, 1999), among others. Theoretical frameworks by researchers including Budyko (1974) and Eagleson (1982) have promoted the study of regional dynamics using low-dimensional modeling techniques. Other studies (Rodriguez-Iturbe et al., 1999; Koster and Suarez, 1999; Fay et al., 2008) have furthered this development; the identification of significant ecohydrologic relationships and responses such as precipitation and water fluxes allows for statistical representation of ecosystem states. Low-dimensional frameworks often are applicable where scarce data availability limits understanding of driving processes and their varying contributions to ecosystems (Bormann and Diekkruger, 2003; Brunsell, 2006). Much is still to be uncovered, however, and the question of small scale (< 100m) interrelationships remains prominent.

Driving relationships provide insight on the dynamic function of water and carbon cycles and can be used as a means to characterize ecosystems. Porporato et al. (2003) used this structure to analyze the precipitation gradient in southern Africa to understand how precipitation translates to small-scale spatial and temporal moisture and vegetation regimes. In Porporato et al. (2003), the identification of major drivers (e.g., gradients, seasonal drought, etc.) offered a framework for analyzing scaled relationships and how the forcings interact with spatial vegetation water availability patterns. This was facilitated by prior work in low-dimensional model developments, which allows for modeling and statistics to replace extensive local data (Guswa et al., 2002; Makela et al., 1996; Rodriguez-Iturbe et al., 2001).

Low-dimensional model outputs and studies have depicted timing and response characteristics of ecosystems and significant research has been conducted in semiarid and forested regions (Laio et al., 2001a; Makela et al., 1996; Porporato et al., 2004).

Probabilistic modeling of external forcing on ecosystem processes soil water flux and precipitation inputs is an important development; studies by Daly and Porporato (2006); Rodriguez-Iturbe et al. (1999); D'Odorico et al. (2000) and others have produced accurate characterizations of hydroclimatic variability from these forcings. Relating water fluctuations and balance (D'Odorico et al., 2000; Daly and Porporato, 2005), carbon fluctuations (Makela et al., 1996), and vegetation productivity and stress (Porporato et al., 2001) provides a strong basis for applying similar frameworks to other ecosystems and other analytical techniques. Studies including those by Brunsell et al. (2009), where energy balance partitioning at different spatiotemporal scales was linked to grassland water and carbon fluxes, and Kleidon and Schymanski (2008), where water budget modeling is applied to thermodynamic optimality and Maximum Entropy Production (MEP) illustrates the robust nature of low-dimensional techniques and possible future uses in ecological modeling.

The objective of this paper is to characterize the ecohydrologic dynamics in the Kansas River Basin by exploring how variation in precipitation impacts evapotranspiration, carbon assimilation, and soil moisture. The specific goals are: (1) to define the roles of timing and magnitude of precipitation as ecological drivers; (2) to better characterize the impacts of changing the timing and magnitude of precipitation on water and carbon fluxes; and (3) to explore these dynamics at the seasonal to annual timescales. Further knowledge about these relationships is crucial for understanding the hydrology and ecology of grasslands and may provide information for future management decisions in the region.

3.2 Site

This study simulates precipitation on an east-west transect across the Kansas River Basin (Figure 3.1). The basin comprises a land area of 155,000 km^2 and encompasses distinct climate, soil, and vegetation gradients. Precipitation ranges from approximately 15 cm $year^{-1}$ in western locations to nearly 100 cm $year^{-1}$ in eastern locations (Lokke and Kidman, 1963), and precipitation timing (λ: events d^{-1}) and magnitude ($\frac{1}{\alpha}$: depth $event^{-1}$) drive local and regional ecohydrology. Basin vegetation types reflect water availability; western locations of the basin tend to have shortgrass species (C_4) that are more drought-resilient while eastern locations' tallgrass and woodland species (C_3 and C_4) require sustained soil moisture (Epstein et al., 1996). The large scale elevation trend is a decrease from west to east, approximately 1820 m to 220 m. Variation in small-scale elevation on the order of tens of meters promotes microclimatic and vegetation variation, such as the extension of woody vegetation westward along low-lying riparian zones. Soils in the Kansas basin tend to have mollic properties, with variations between sand, silt, and clay composition, along with vegetation rooting, forming differences in active soil depth. Land cover change has been drastic in the basin under European influence and land management continues to change land classes. In 2001, the National Land Cover Dataset (NLCD) classified land use in the basin as 49% cultivated, 39% grassland, 4.4% developed, and 2.4% forest.

The Kansas River basin is also likely to be impacted by climate change. Global Climate Model (GCM) forecasts for the region indicate an increase in surface temperature and a mean decrease in precipitation from the IPCC A1B scenario (Brunsell et al., 2010). Precipitation levels are expected to decrease slightly in every season except winter, with the greatest decreases occurring in western locations during summer months (Brunsell et al., 2010). These changes are expected to result in in-

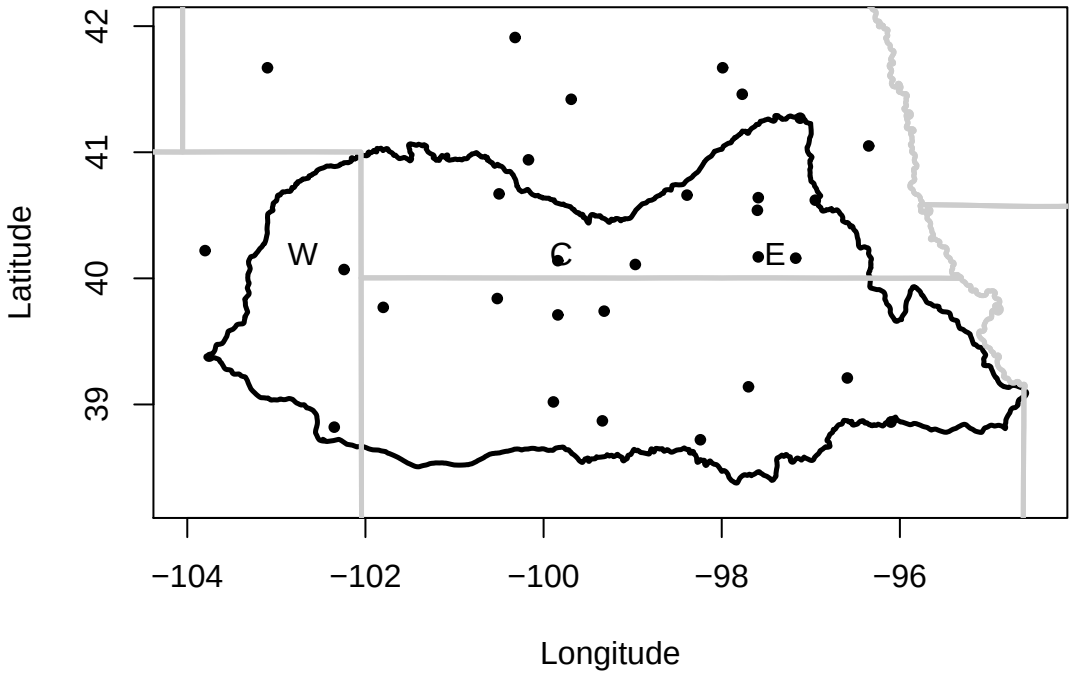

Figure 3.1 Kansas River basin USHCN station locations. Western (W), central (C), and eastern (E) basin locations are indicated for reference.

creased summer evapotranspiration and may therefore increase agriculture irrigation needs and shift grassland vegetation towards C_4 and other drought-resilient species (Brunsell et al., 2010). The spatial and temporal dynamics of climate change have not yet been evaluated for ecohydrologic dynamics across land classes in the Kansas basin beyond that of Brunsell et al. (2010), but it is possible that climate change will have profound effects on agricultural practices and the viability of some vegetation classes.

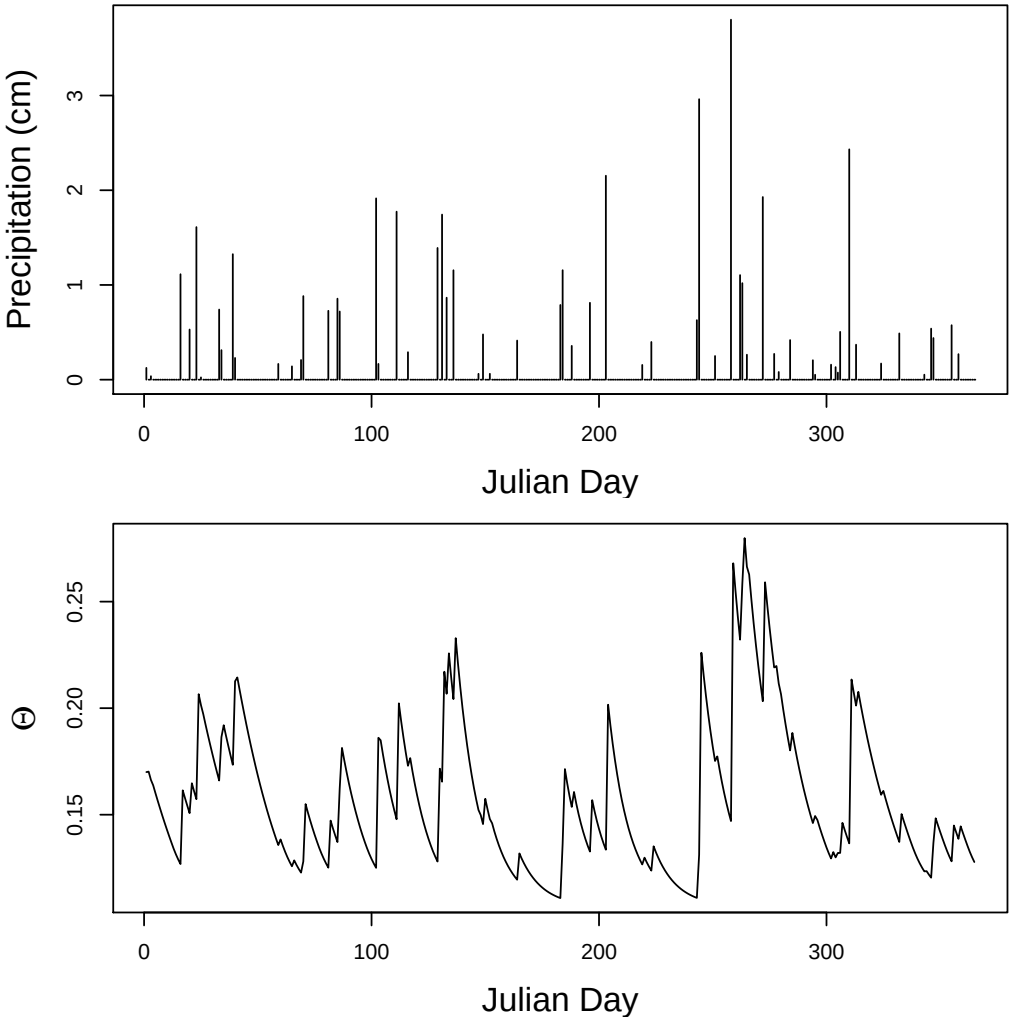

Figure 3.2 Modeled (top) precipitation and soil moisture for one year.

3.3 Methods

To explore potential states of grassland ecosystems, we focus on accurate characterization of precipitation (P), soil moisture (θ), evapotranspiration (E), and carbon flux (A) dynamics. This characterization illustrates the unique ecohydrological roles of state variables and fluxes as they potentially exist across space and time.

3.3.1 Precipitation dynamics in the Kansas River basin

Precipitation timing and magnitude were calculated for 30 sites across the Kansas basin transect using United States Historical Climatology Network (USHCN) daily precipitation data (Williams Jr et al., 2006) [*http* : *//cdiac.ornl.gov/epubs/ndp /ushcn/usa.html*]. Data records from individual stations ranged from 49 to 120 years in length. The transect was located from -96° to -105° W Longitude and 38.5° to 42° N Latitude (Figure 3.1). Site data were used to calculate mean λ and α values from precipitation datasets, where λ is calculated from a Poisson distribution of the timing of days with a precipitation event and α is calculated from an exponential distribution of the magnitude of these events.

Precipitation was modeled as a Poisson process of event timing (λ) with random, exponentially distributed mean depth ($\frac{1}{\alpha}$), and daily values are generated as a Monte Carlo process from interaction of λ and α (D'Odorico et al., 2000). Events are modeled at the daily timescale and are considered instantaneous. A sample year of stochastic P and θ response is seen in Figure 3.2.

Simulations consist of precipitation implementation within a low-dimensional modeling framework to output daily θ, daily E and daily A values for a timespan of 1200 years. Daily values are shaped by potential evapotranspiration (E_p) [cm day^{-1}], soil type, and vegetation water use efficiency (WUE). Water use efficiency is treated as

Table 3.1 Model parameterizations

Parameter	Value	Units
ψ	-.0007	MPa
b	4.9	n/a
c	12.8	n/a
K_s	80.0	cm d^{-1}
n	0.43	n/a
β	13.8	n/a
θ_h	0.107	m^3 m^{-3}
θ^*	0.40	m^3 m^{-3}
θ_{fc}	0.50	m^3 m^{-3}
nZr	17.0	m^3 m^{-2}
E_w	0.05	cm d^{-1}
WUE	0.49	$\frac{molC}{cmE}$
E_{max0}	0.35	cm d^{-1}
δ_{et}	0.50	n/a
ψ_{et}	2.618	d^{-1}
ω_{et}	0.0172	n/a

an upper bound to carbon assimilation and not as a major scaling factor in order to facilitate the relation of carbon assimilation to evapotranspiration. Atmospheric, soil, and vegetation values were held constant across the sites to remove their effects on model outputs. These values are available in Table 4.1.

3.3.2 Water and carbon fluxes

Daily potential evapotranspiration E_p was calculated from Milly (1994) as:

$$E_p = (E_{p0}/nZr) \cdot [1 + \delta_{et} \cdot sin(\omega_{et} \cdot h_{day} + \phi_{et})] \tag{3.1}$$

Where E_{p0} is mean annual E_p, nZr is the active soil depth [cm], δ_{et} is the amplitude about $\frac{E_{p0}}{nZr}$, ω_{et} is the frequency of the sinusoid [d^{-1}], h_{day} is the hydrologic day, and ϕ_{et} is the phase shift. Actual evapotranspiration [cm d^{-1}] is calculated by implementing a soil moisture limitation on E_p by a piecewise manner from Laio et al. (2001b):

$$
\begin{aligned}
if \quad 0 < \theta \leq \theta_h; \quad & E = 0 \\
if \quad \theta_h < \theta \leq \theta_w; \quad & E = E_w \cdot ((\theta - \theta_h)/(\theta_w - \theta_h)) \\
if \quad \theta_w < \theta \leq \theta^*; \quad & E = E_w + (E_p - E_w) \cdot ((\theta - \theta_h)/(\theta_w - \theta_h)) \\
if \quad \theta > \theta^*; \quad & E = E_p
\end{aligned}
\tag{3.2}
$$

Where θ is volumetric soil moisture [m^3 m^{-3}], θ_h is the hygroscopic point, θ_w is the wilting point, E_w is evapotranspiration at wilting point [cm d^{-1}], and θ^* is the reduction point.

To couple the water and carbon fluxes, we calculate maximum carbon assimilation (A_{max}) [mol m^{-2} d^{-1}] as:

$$
A_{max} = E_p \cdot WUE \tag{3.3}
$$

Actual carbon assimilation is calculated according to Daly and Porporato (2005):

$$
\begin{aligned}
if \quad \theta \leq \theta_w; \quad & A = 0.0 \\
if \quad \theta_w \leq \theta < \theta^*; \quad & A = (\tfrac{\theta - \theta_w}{\theta^* - \theta_w}) \cdot A_{max} \\
if \quad \theta \geq \theta^*; \quad & A = A_{max}
\end{aligned}
\tag{3.4}
$$

We focus on soil moisture, evapotranspiration, and carbon assimilation to characterize the responses to variation in precipitation forcing events as parameterized by λ and α.

3.3.3 State space and Budyko analysis

Analysis of the precipitation state space promotes the identification of relationships between precipitation (λ and α) and surface responses (θ, A, and E). In this case, we model θ across possible iterations of λ and α and under differing E_p regimes. Precipitation λ and α values corresponding to averages for western, central, and

eastern locations of the Kansas basin transect result in differing θ, E, and A conditions due to E_p variation. Timing and magnitude values for these are mean values from USHCN sites nearest to a corresponding longitude point (-101° W Longitude for western, -98.5° W Longitude for central, and -96° W Longitude for eastern, Figure 3.1).

We assess the effects of variation in precipitation timing and magnitude on water fluxes using Budyko (1974) dryness (ϕ) and evaporative (ε) metrics. These illustrate land-atmosphere interactions and the sensitivity to precipitation forcing and potential evapotranspiration, and evolve over time in response to variation in these variables. The dryness metric is a relation of E and P in determining gains and losses in soil moisture and is calculated as:

$$\phi = \frac{E}{P} \tag{3.5}$$

and ε is a relation of actual to potential evaporative fluxes calculated using:

$$\varepsilon = \frac{E}{E_p} \tag{3.6}$$

3.4 Results

3.4.1 Soil moisture dynamics in precipitation state-space

The interaction of precipitation and evapotranspiration is important in assessing soil moisture dynamics for different values of potential evapotranspiration and precipitation timing and magnitude. The impacts of λ and α on annual $\overline{\theta}$, how E shapes $\overline{\theta}$, and how λ, α, and E interact in terms of surface hydrology are shown in Figure 3.3. The top frame illustrates soil moisture values across λ and α for E_p levels of $\frac{1}{2}$ their

expected levels ($E_{po} = 0.17$ cm d^{-1}), the middle illustrates these for expected E_p ($E_{po} = 0.35$ cm d^{-1}), and the bottom illustrates the these for 2 times their expected levels ($E_{po} = 0.69$ cm d^{-1}). Greater range of $\overline{\theta}$ across the horizontal axis suggests that variation in precipitation timing impacts θ to a great degree. This effect seems to diminish in lower $\overline{\theta}$ conditions, illustrated by the nature of the contour lines; vertical lines display a decreased sensitivity to event magnitude, while a horizontal shift displays increasing sensitivity to α as it increases, decreasing average event magnitude.

Actual evapotranspiration also shapes mean annual soil moisture. Variation in E_p directly impacts annual $\overline{\theta}$ states through actual evapotranspiration and promotes deviation in θ sensitivity to λ and α (Figure 3.3); $\frac{1}{2}$ E_p increases $\overline{\theta}$ and increases sensitivity to event magnitude, while $2 \cdot E_p$ decreases $\overline{\theta}$ and increases sensitivity to event timing. These drier and wetter states experience differing sensitivity of λ and α, resulting from variation in E_p scaling $\overline{\theta}$ conditions, although specific combinations of λ and α may show no apparent change in sensitivity for differing θ states.

The roles of precipitation timing and magnitude, and potential evapotranspiration exhibit unique traits within the Kansas River basin, as shown in Figure 3.3. Points (from left to right, descending) correspond to timing and magnitude values in western ($\lambda = 0.16$; $\alpha = 1.35$), central ($\lambda = 0.20$; $\alpha = 1.15$), and eastern ($\lambda = 0.24$; $\alpha = 1.10$) basin locations. Precipitation variance results in differences in $\overline{\theta}$ across locations varying from approximately 0.34 in eastern locations to 0.26 in western locations for normal E_p with a field capacity (θ_{fc}) of 0.50. In all plots, however, sensitivity to λ and α varies little under differing $\overline{\theta}$ states. This suggests that, on the annual timescale, λ and α have similar sensitivity across the basin, although the role of event timing is slightly greater than that of magnitude for a constant E_p, as shown by greater distance between α contours than λ and suggesting greater change in θ to percent changes in λ than α.

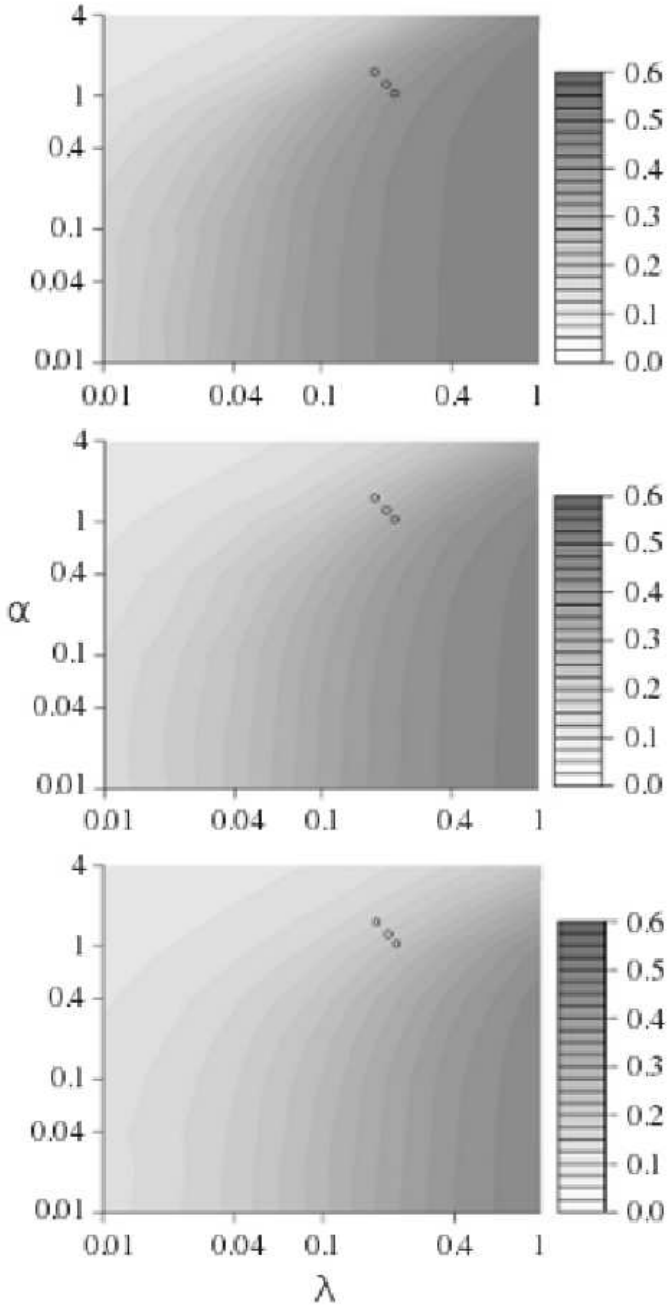

Figure 3.3 Mean annual soil moisture across λ and α space for varying $\overline{E}_p$ regimes. (top) $\overline{E}_p = 0.17$; (middle) $\overline{E}_p = 0.35$; (bottom) $\overline{E}_p = 0.69$ values correspond to western, central, and eastern Kansas basin locations and are denoted by points on the plot.

3.4.2 Budyko plots

Budyko plots presented in Figure 3.4 display mean annual dryness and evaporative metrics across 9 combinations of 3 timing (λ = 0.125, 0.5, 1.0; rows) and magnitude (α = 0.5, 2.0, 4.0; columns) values, the range of which is expected to encapsulate all probable precipitation variation for the central United States. This range extends from wet annual conditions ($\lambda = 2.0$; $\alpha = 0.5$) to dry ($\lambda = 0.125$; $\alpha = 4.0$). All points are mean daily values from 1200 years of simulation; maximum ε values exist in fall and winter and evolve towards drier conditions, reaching highest ϕ and lowest ε in summer. E_p (0.5 cm d^{-1}) shapes ϕ to a great degree; its seasonal increase drives E and helps create differences in ϕ and ε.

Differences across the plots represent the impact of precipitation timing and magnitude variation on soil moisture and water fluxes. While E and P have distinguishable roles in producing ϕ and ε metrics, their nonlinear interaction produces conditions that are not easily attributed to either variable. General trends, however, are illustrated. Decreasing timing shows an increase in ϕ, a lower minimum ε, and a temporally shorter period of maximum ε in the winter and a longer period in the summer. This is expected: decreasing λ increases time between events and overall precipitation amounts; this reduces average θ values. Increasing α decreases event magnitude and increases ϕ throughout the year. The increase of α when $\lambda = 0.5$ and 0.125 is illustrative of this; drier conditions increase ϕ and decrease maximum and minimum ε.

All plots have some degree of hysteresis, defined here as differing ϕ for the same ε between the early and late growing season, although this is not always realized. Hysteresis between spring and fall Budyko metrics is caused by winter soil moisture recharge maintained into early spring, visible as ε maxima as ϕ values increase. The fall season, however, follows a period of high evapotranspiration and ϕ, resulting in

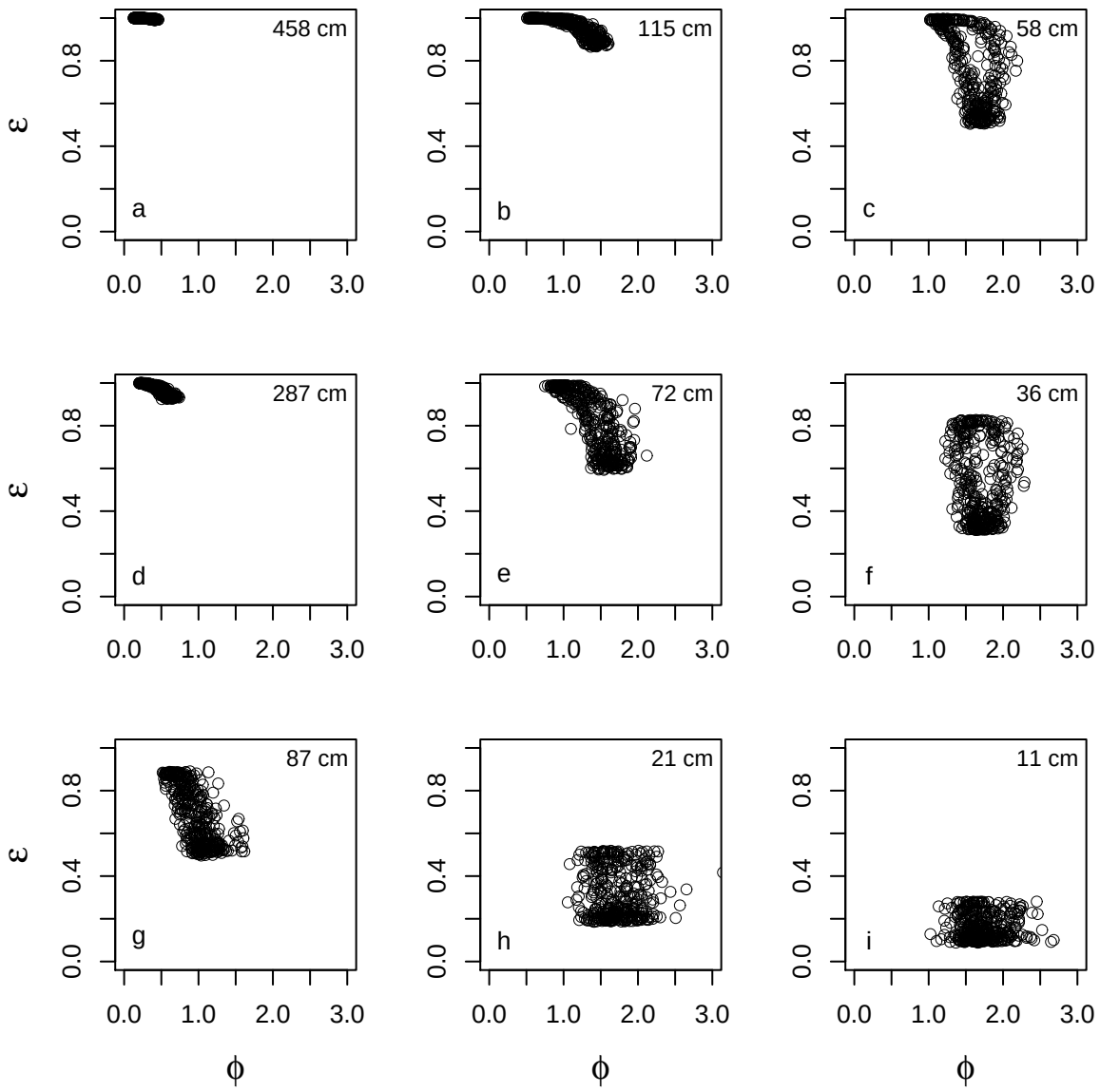

Figure 3.4 Budyko analysis of ecosystem dryness (ϕ) and evaporative (ε) metrics on an annual scale. Metrics are plotted across λ and α space: $\lambda =$ 0.125, 0.5, and 1.0 from bottom to top; $\alpha = 0.5$, 2.0, and 4.0 from left to right. Mean annual precipitation is shown in the upper right corner of each plot.

lower ε values until ϕ decreases. Winter θ recharge ensures that all realizations experience hysteresis-causing conditions, although hysteresis is not well-defined in cases where P variance produces θ values that are too high or low to show much variation between spring and fall. Hysteresis may be best observed where E_p and precipitation variability have equal effects on θ conditions. The breakdown of hysteresis is not understood, except in plot i, where dryness is expected to dominate θ conditions. Additionally, as α increases and $\lambda = 1.0$ in plots a, b, and c, maximum ε is not decreased due to high λ values, even under drier winter conditions.

The individual roles of λ and α can be explored in Figure 3.4. Plot a illustrates a reduction in ε due to a fourfold increase in α (decreased event magnitude) in plot b and a fourfold decrease in λ (increased time between events) in plot d; increasing α results in a greater decrease in both ϕ and ε compared to the decrease in λ. Plots c, e, and g also illustrate this, but are complicated by changes to both timing and magnitude. Plot e appears to exist as a midway point between c and g and has similar seasonal dynamics to both. Plot c, which introduces a doubling of α and halving of λ, results in greater ϕ and lower ε in the summer, as well as broader hysteresis between spring and fall seasons. The evaporative metric maintains a winter maximum for longer in this case. In plot g, which halves λ and α, the range of ϕ and ε values are similar to plot e, but with a lowered winter ε maxima and a summer minima similar to plot c. All of these exhibit differences in seasonal θ availability from similar timing and magnitude impacts on annual $\overline{P}$; doubling α produces a 50% reduction of $\overline{P}$ and halving λ reduces $\overline{P}$ by 40%. Variation in ϕ and ε, however, bear slight resemblance to $\overline{P}$ values but are scaled by soil moisture and evapotranspiration at the daily and seasonal timescales. This stresses the importance of the small-scale, nonlinear interaction between λ and α in producing ecosystem conditions instead of relying on large-scale trends and relationships.

3.4.3 Annual water and carbon dynamics

Figure 3.5 shows the ensemble daily means and variances of soil moisture, evapotranspiration, and carbon assimilation for western ($\lambda = 0.16$, $\alpha = 1.35$), central ($\lambda = 0.20$, $\alpha = 1.15$), and eastern ($\lambda = 0.24$, $\alpha = 1.10$) locations in the Kansas basin. Annual dynamics of $\overline{\theta}$ vs. $\overline{E}$ have a counterclockwise annual cycle from greatest to least soil moisture. Eastern locations of the basin display the highest values of $\overline{\theta}$ and $\overline{E}$, followed by central locations, and then western locations. This hierarchy is preserved in annual range of $\overline{\theta}$ and $\overline{E}$ values as well. All locations experience the same general trend: a spring buildup of $\overline{E}$ from high $\overline{\theta}$ and increasing E_p, a summer drydown of $\overline{\theta}$ due to E_p, and an increase of $\overline{\theta}$ during winter months as E_p declines.

Daily ensemble variance of soil moisture (σ_θ^2) and evapotranspiration (σ_E^2) is displayed in the upper right plot of Figure 3.5. Annual cycles of eastern and central locations move in a clockwise manner from lowest σ_E^2 in winter to highest in summer, while western locations have highest σ_θ^2 in winter. Eastern basin locations experience the highest summer and lowest winter soil moisture and evapotranspiration variance. Central locations have higher σ_θ^2 than eastern locations in every season but summer, and show greater response to σ_θ^2 fluctuations in the spring due to their lower $\overline{\theta}$ values during this time; lower $\overline{\theta}$ values exist during the drier, more stable, fall season. Eastern locations experience their highest σ_θ^2 later in the spring. Central locations are less variable than eastern for σ_E^2 in all seasons except winter. Western locations' σ_θ^2 and σ_E^2 values show reduced $\overline{\theta}$ in the spring, summer, and fall, and decreasing σ_θ^2 and increasing σ_E^2 in the summer. This is due to summer drydown producing low, stable values of $\overline{\theta}$, and winter conditions making soil moisture reliant on precipitation events. All locations have high $\sigma_{\overline{E}}^2$ in summer due to high E_p values driving E to a great degree, while $\sigma_{\overline{\theta}}^2$ values are more stable. As in the upper left plot, the greatest overall σ_θ^2 and σ_E^2 range is in eastern locations, although these experience the lowest

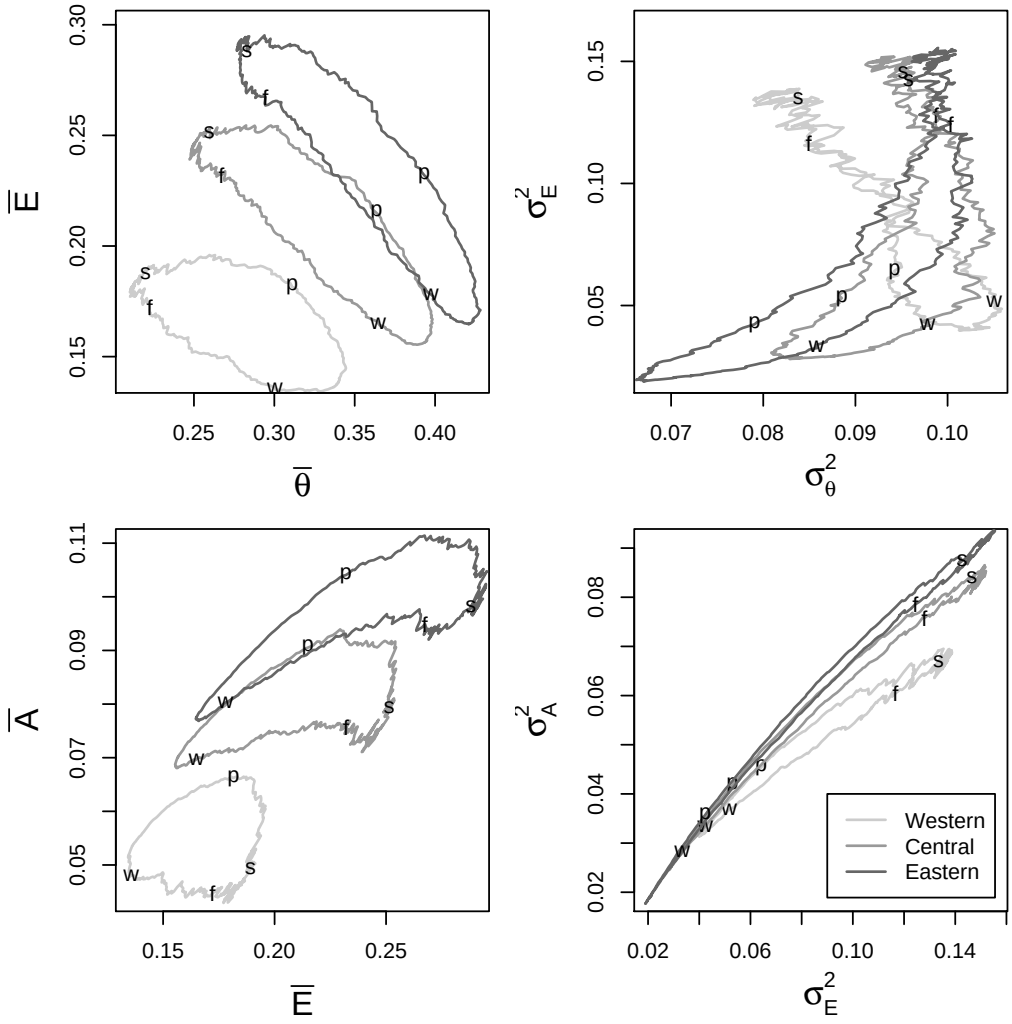

Figure 3.5 Mean daily θ, E, and A and variance (western: $\lambda = 0.16$, $\alpha = 1.35$; central: $\lambda = 0.20$, $\alpha = 1.15$; eastern: $\lambda = 0.24$, $\alpha = 1.10$). For reference, seasons are denoted as winter = w, spring = p, summer = s, and fall = f.

$\overline{\theta}$ variance in spring and fall.

The lower left plot expresses daily values of mean evapotranspiration vs. mean carbon assimilation. Eastern locations experience highest ensemble $\overline{E}$ and $\overline{A}$ values and greatest overall range, followed by central and western locations, respectively. The unique feature of this plot is summer drydown, which reduces $\overline{A}$ for western and central locations of the basin with very little change in $\overline{E}$, while eastern $\overline{E}$ and $\overline{A}$ reach a higher summer value and decrease in a more direct manner. It is also important to note that summer drydown is lessened by E_p but $\overline{A}$ is lagged from this due to lowered θ conditions.

The variance of evapotranspiration and carbon assimilation have a counterclockwise annual cycle (Figure 3.5, bottom right). Eastern locations have the greatest range of σ_E^2 and σ_A^2, followed by central and western locations. Both eastern and central locations of the basin are similar, with eastern locations having higher σ_E^2 and σ_A^2 in all seasons except winter, where θ is expected to be stable. Summer drydown decreases σ_E^2 and σ_A^2 in central and western locations due to low soil moisture; this also induces σ_A^2 hysteresis in western locations. These differences reflect the relation between precipitation and evapotranspiration; eastern locations experience the highest precipitation and, therefore, highest θ recharge in winter when E_p is low and highest evapotranspiration in the summer due to highest θ availability. This is reflected in low winter θ variance and high summer σ_E^2 and σ_A^2. Western portions experience the opposite effect; low precipitation levels are most affected by winter evapotranspiration (highest variance) and have the least impact on increasing E during summer months (lowest variance). In this case, ecosystem stability can be a product of θ surplus or deficit and is directly related to E and A values.

3.5 Discussion

Precipitation variance drives soil moisture characteristics through nonlinear interactions of event timing and magnitude. From Figure 3.3, the variability in mean annual $\overline{\theta}$ along the horizontal axis suggests the role of λ is greater than α in producing mean annual conditions, but this role is diminished as α increases and the role of λ and α begin to have similar weight, as seen by the decreasing vertical nature of contour lines between θ ranges. This is expected because high event magnitude (low α) is reliant on timing between events for producing annual $\overline{\theta}$ conditions, and vice versa. This dynamic may only hold where extremes in annual $\overline{\theta}$ values exist. Annual $\overline{\theta}$ conditions in the Kansas basin are not indicative of differing λ and α weights, but show that λ and α weight varies for differing θ conditions. In addition, annual $\overline{P}$ and $\overline{\theta}$ do not always correlate to λ and α values. an extreme example is the case of $\lambda = 0.1$ and $\alpha = 0.1$ vs. $\lambda = 4.0$ and $\alpha = 1.0$, where annual $\overline{P}$ is 352 and 358 cm, respectively, but annual $\overline{\theta}$ varies from 0.34 to 0.49, a difference of 31%. Lesser examples also exist across $\overline{P}$ and $\overline{\theta}$ for differing λ and α, suggesting that ecosystem water flux is more sensitive to small temporal variability and that ensemble averages, while able to illustrate gross differences in ecosystem states, are not able determine the roles of shorter temporal-scale forcings.

Soil moisture seasonality is a product of the interrelation between precipitation variance and evapotranspiration at the daily timescale. Seasonal E_p drives θ availability, with a negative relationship between E_p and θ. E_p fluctuations, however, have no effect on the statistical properties of θ (Daly and Porporato, 2006), which maintains the interrelation of λ and α within θ states. Therefore, θ is a product of seasonal E_p and P, but the sensitivity of θ to percent changes in λ and α is variable and dependent on daily θ values. This is evident in Figure 3.3, where the percent

change from 0.04 to 0.1 and 0.4 to 1.0 for λ and α produces varied annual $\overline{\theta}$ responses. How this sensitivity translates to mean daily values is important; temporal averaging of stochastic precipitation maintains the same average ensemble relationship between precipitation timing and magnitude and E_p, although actual relationships are highly variable at the daily timescale. Combinations of λ and α within similar θ state space, such as Kansas basin locations in Figure 3.3, maintain average ensemble weight between λ and α for varying E_p regimes and differences in $\overline{\theta}$ between the locations are a product of λ and α variance (Daly and Porporato, 2006). Temporal scales of interaction are important for translating the high daily variability of state processes to ensemble averages, and suggests that important ecosystem dynamics such as water availability and evapotranspiration have differing roles depending on the temporal scale of analysis.

Sensitivity of soil moisture to variable timing and magnitude across the year illustrates variation in water fluxes and potential evapotranspiration's effects on timing and magnitude relationships. Figure 3.4 illustrates this for a range of λ and α combinations bounded by possible extremes of wet and dry ecosystem moisture regimes. Variance in λ or α can individually increase or decrease θ, influence ε and ϕ metrics, and promote annual scaling towards wet and dry conditions. Seasonality in ε and ϕ across λ and α, however, suggests the manner in which λ and α create θ is more complex. Differences across winter soil moisture recharge and summer drydown, and spring and fall hysteresis all illustrate the dynamics of λ and α seasonality, and variation in ε and ϕ within these phenomena hint at varying λ and α sensitivity. For the Kansas basin, the roles of λ and α are multi-faceted; each has a daily sensitivity contingent on θ conditions, a seasonal sensitivity to seasonality in θ and ecosystem function, and an ensemble sensitivity for scaling the ecosystem towards a preferred moisture regime.

The general trend of Figure 3.4 is a decrease in available soil moisture from upper left to lower right, with the driving mechanisms being a decrease in event timing from top to bottom and an increase in event magnitude from left to right creating varying seasonal states of increased dryness. As drier conditions evolve across λ and α, a number of trends develop. Periods of θ recharge, caused by seasonality in E_p and resulting in high ε values and low dryness, is driven by λ given adequate α (Rodriguez-Iturbe et al., 1999). Reduction in maximum ε occurs at a lower ϕ for λ variation, while summer drydown is more affected by α, showing greater dryness and greater reduction in ε. Evapotranspiration decreases θ conditions from spring to summer, increasing the impact of α on ecosystem dryness and evaporative function, and increases θ in fall and winter, increasing the effect that λ has on decreasing dryness and increasing ε. Seasonality in dryness is illustrated by hysteresis between spring and fall, caused by winter θ storage lessening spring ϕ and θ variance and summer drydown increasing fall ϕ and θ variance. The roles of precipitation timing and magnitude are important as well; decreasing λ promotes less hysteresis between spring and fall, lower ϕ, and lower ε range while increasing α produces more hysteresis, greater overall ϕ, and greater ε range. Seasonality of E_p scales towards wet or dry θ states and promotes different sensitivities to λ and α which translate to variance in daily (and therefore ensemble) θ and varied ε and ϕ states. In cases of intermediate precipitation variance, ecosystems are characterized by wet and dry periods, with the spring and fall seasons existing as transitional periods of low and high variance in moisture and E, respectively, with deviations across λ and α scaling θ states towards greater wetness, dryness, or seasonality between the two.

Variance in ε and ϕ illustrates the importance of seasonality on ecosystem water flux dynamics and when and to what degree deviations from mean ecosystem states are likely to occur. Figure 3.4 shows less uniformity in ε and ϕ for spring and fall

as λ and α promote lower θ, related to higher seasonal σ_θ^2 in Figure 3.5. Winter ε maximization suggests sufficient θ storage to reduce variance in ε and ϕ in the spring, but lowered ε lessens the effect of winter θ storage on water flux in all seasons. It also follows that fall variance in ε and ϕ is greater than spring for all realizations as precipitation timing and magnitude have a greater effect on water flux in absence of θ storage. Both wet and dry λ and α conditions produce little seasonal variation in ε, while ϕ may show greater variation, as illustrated best for wet conditions in the upper left plot.

Coupling of soil moisture to Kansas River basin seasonality produces daily variation in state variables that deviate from ensemble averages. Seasonality in soil moisture and evapotranspiration variance are important for assessing how much daily variation exists for these variables, when this variation occurs, and if this might inhibit ecosystem function. Both are characterized by wet and dry seasonality except for the western location, where summer drydown decreases σ_θ^2. Evapotranspiration is not maximized during the growing season due to its coupling to P, resulting in high daily θ variance and low summer θ range. Soil moisture variance is highest in the fall due to increased dependence on precipitation, but lessens as evaporation decreases. Winter and spring σ_θ^2 is dependent on fall and winter recharge, respectively, and variance is lowest where λ and α produce the highest daily $\overline{P}$. Central and eastern locations of the Kansas basin are similar in their seasonal soil moisture structures. The eastern location has higher water fluxes and variance corresponding to higher λ and lower α values, while the western location is more influenced by summer drydown and exists with much drier seasonal θ conditions and an altered tendency towards higher winter and lower summer ε and ϕ variance.

Mean daily model outputs (Figure 3.5) for the Kansas basin show similarities to variance plots and support precipitation timing and magnitude roles. Daily water

and carbon fluxes correlate to expected λ and α roles for $\overline{\theta}$ conditions and evolve similar to E_p seasonality, with some temporal deviation in ensemble averages. Western locations show minimized seasonal dynamics due to decreased θ availability and have the lowest range of θ, E, and A values. Winter θ storage is best illustrated by E vs. A, where winter is the maximum period for all locations. Water limitation is evident in this plot as well; A has the greatest values in all locations for seasonal periods of greatest θ and shows greater variance during the drier fall season than the wetter spring. The effect of dryness is also evident where the eastern location has greater overall carbon flux than drier locations, and where its correlation between ensemble σ_E^2 and σ_A^2 is maintained at a lower level in the spring. Here, σ_E^2 and σ_A^2 increases with increasing E_p, but locations with greater daily $\overline{P}$ have greater variation in water and carbon fluxes, indicating that, in the Kansas basin, water limitation plays a primary role in ecosystem state processes, especially in the summer and fall seasons. Precipitation variation plays the primary role in all seasons except winter, where processes are limited by phenology and E_p. Global climate change could affect precipitation timing and magnitude and potential evapotranspiration across seasons in the Kansas basin (Brunsell et al., 2010), disrupting ecosystem water and carbon cycling. The implications of this are yet unknown; the net effect of disruptions is contingent on soil and vegetation properties, the nature of local changes to precipitation and potential evapotranspiration and, in the case of agriculture, the availability of groundwater reserves locally and where upwind soil moisture-precipitation feedbacks may exist (Jones and Brunsell, 2009).

Sensitivity to precipitation variance is a major driver of grassland processes. Sensitivity to λ and α is scaled by daily θ conditions and E_p trends, which feedback on θ availability and the roles of λ and α in creating θ states. Temporal scaling is important; representation of daily through annual timescales provides informa-

tion on how ecosystem states evolve, how they may be impacted by regional climate changes, and how spatial scaling might best represent ecosystem dynamics as they evolve over time and under varied conditions. As a whole, precipitation variance and potential evapotranspiration are good indicators of ecological function and may have additional value at the daily, seasonal, and longer timescales. This is illustrated by annual values of soil moisture being a product of interactions at different temporal scales. Soil moisture can indicate annual impacts of event timing and magnitude effects, the seasonality of potential evapotranspiration driving ecosystems between periods of moisture availability and related sensitivities to precipitation, and daily fluctuations in drivers and state processes. These suggest trends in seasonal ecologic stability and flux. Ecosystem dynamics are closely correlated to water and carbon fluxes through soil characteristics and the water use efficiency, and variation can be explored in terms of flux dynamics and preferred ecosystem states.

Future analysis could benefit from incorporating seasonality of precipitation forcing to the framework of process characterization and temporal analysis presented here. Grassland ecosystems are driven by seasonal variance in λ, α, and E_p, but their in-situ translation of these is highly dependent on heterogeneous soil and vegetation and the evolved relationships between these and the local moisture regime. In addition, future changes to P and temperature from climate change may alter the nature and roles of P and E for grassland ecosystems (Brunsell et al., 2010). The way these changes translate across spatial and temporal scales is important; the impact of variability has differing roles based on how and where variability occurs and in what direction the moisture regime shifts towards. Understanding how P variance evolves and creates annual variation in ecosystem processing is an important part of accurate representation of current and future grassland function in the Kansas basin region and we hope it will aid in the directed, contemplative assessment of the ecosystem as

a dynamic resource for the present and future.

Chapter 4

Climate Change Drives Grassland Fluxes

Climate change may have profound impacts on the ecology and hydrology of grassland ecosystems. Changes in climate forcings such as precipitation (P) and potential evaporation (E_p) may alter ecosystem flux dynamics and shift functioning away from stable values. It is important to understand how climate forcings and resulting fluxes exist across different levels of support, and how they scale to long-term ecosystem states. Forcings such as precipitation and solar radiation play critical roles in creating the spatial and temporal heterogeneity of landscapes and are shaped by influences including feedbacks and biotic processes (Claussen et al., 2001; Ivanov et al., 2008). Understanding the way changing climate might alter this interplay is important for assessing future ecosystem functioning.

Exploring forcing mechanisms and variable responses aids in assessing the biotic system functioning. Examples are widespread for semiarid ecosystems and include research in many disciplines. Of these, the relation of processes at different timescales and sensitivities is of particular importance (D'Odorico et al., 2000; Laio et al., 2002;

Daly and Porporato, 2006). Studies include moisture allocation during drydown periods (Teuling et al., 2006,b; Milly, 1994), plant-scale analyses of C_3 and C_4 photosynthesis (Vico and Porporato, 2008), and water flux coupling to surface processes (Ridolfi et al., 2000a). Similar approaches have been used to assess seasonal sensitivities of mass and energy fluxes to climate forcings as a way of characterizing ecosystem processes (Daly and Porporato, 2006; Petrie and Brunsell, 2010). Representation of feedbacks and atmospheric coupling extend this characterization further (Brunsell and Gillies, 2003); defining the scales of ecosystem functioning aids in more-directed application of processes and variability.

The relationships governing nonlinear surface processes may be assessed using low-dimensional modeling techniques. The strength of low-dimensional modeling is accurate representation of major ecosystem forcings as the framework of ecosystem flux dynamics. Low-dimensional models have been applied to precipitation and water flux variability (Daly and Porporato, 2005, 2006; Koster and Suarez, 1999) and also to spatiotemporal water-limitation and flux depression (Ridolfi et al., 2000b; Porporato et al., 2001). They have also been used to identify how relationships between vegetation and environment govern spatial vegetation patterns in the Kalahari grassland in Southwest Africa (Caylor and Rodriguez-Iturbe, 2003; Porporato et al., 2003) and hydrology of the Konza prairie in North Central Kansas (Porporato et al., 2004). Recently, the authors used a similar low-dimensional technique to represent major ecohydrologic relationships across the Kansas River Basin precipitation gradient (Petrie and Brunsell, 2010). Further studies have extended low-dimensional analysis to gas exchange models (Vico and Porporato, 2008), and similar techniques may find use in optimality hypotheses and thermodynamics.

Mesic grasslands exhibit dynamic responses to climate. Variation and disturbance are, in many ways, normal for grasslands and the resulting heterogeneity across levels

of support is an important component of these ecosystems' functioning (Knapp et al., 1998; Collins et al., 2002). Local ecology also feeds back at these differing scales, producing specialized function and niche development (Collins et al., 2002). The ecologic role of vegetation, for example, is one of many parts. It is affected by forcings, feedbacks on them, and changes in response over time. Water and carbon fluxes are products of these processes and can be upscaled to represent large-scale ecosystem responses (Betts et al., 1997). Photosynthesis, for example, varies in sensitivity to precipitation at different states of water limitation and can be modeled to assess likely periods of soil moisture limitation (Petrie and Brunsell, 2010). How overall effects are realized is of interest both for the natural resource value of grasslands and their susceptibility to species and habitat loss.

Variability in water-use efficiency (WUE, $\frac{\delta A}{\delta E}$ is the slope of the assimilation-evaporation curve (mmol A mol E^{-1})) is a product of varying sensitivities of stomatal conductance to surface temperature, vapor pressure, and seasonal phenology (Monson et al., 1986; Nippert et al., 2009). The effect of variable water-use efficiency is differences in carbon assimilation patterns between vegetation species and C_3 and C_4 classes (Epstein et al., 1996; Emmerich, 2007). Benefits from maintained photosynthesis during dry, warm summers (Monson et al., 1986; Nippert et al., 2007; Niu et al., 2005) and mild, wet springs vary across phenologies (Vermeire et al., 2009) and may be negated in cases of water or nutrient limitation, even under an enhanced early growing season (Makela et al., 1996; Niu et al., 2005; Nippert et al., 2007). How these periods affect long-term grassland species composition and interaction is less well-defined. Stress effects vary between species and, although ecosystem compositions reflect, for example, moisture dynamics, neither the C_3 or C_4 photosynthetic pathway appears to define the dynamics of its vegetation subset (Nippert et al., 2007). Water-use efficiency measurements and simulations reflect these nonlinearities inten-

tionally and unintentionally; water-use efficiency responds more to variation in soil moisture than photosynthetic pathway or phenology, although it encompasses all of these. How metrics of analysis represent vegetation versus environment is a grey area in understanding landscape-scale ecosystem dynamics. Many of these metrics, however, do provide useful quantification of processes within the limitation of their definition (Emmerich, 2007).

Global Climate Model (GCM) projections for the central United States were evaluated by Brunsell et al. (2010) for the International Panel on Climate Change (IPCC) A1B climate change scenario. Central Plains ecosystems are projected to experience an increase in mean surface temperature and higher precipitation variability (fewer events, but with higher magnitude), with slightly decreased mean annual precipitation (Brunsell et al., 2010). These compliment other projections for the Central Plains (Houghton, 2001). Studies by Richardson et al. (2009) and Monson et al. (2005) have explored earlier onset conditions for temperate Harvard and arid Colorado forests; results suggest differing ecosystem and water availability responses to earlier growing season onset including heightened spring productivity and increased summer drydown. Induced seasonality between temporal periods of the growing season might be an important diversifying selector in mesic grasslands, an intermediate between the temperate east and arid west. Long-term effects on ecohydrologic dynamics are expected to reflect increased short-term variability of soil moisture, and also increased seasonality between early-season productivity and summer drydown (Angert et al., 2005).

To explore potential states of mesic grasslands under changing climate, we focus on the effects of increased precipitation variability, earlier growing season onset, and heightened potential evaporation on seasonal water flux dynamics, growing season length, and carbon assimilation for semiarid forb and grass species. Specific goals

are: (1) To characterize the individual and aggregate effects of decreased precipitation timing and increased magnitude, heightened potential evaporation, and earlier growing season onset on carbon assimilation, soil moisture, and growing season length; (2) to determine how seasonality in water-use efficiency shapes the vegetation response to changing climate; and (3) to explore carbon assimilation responses of vegetation classes and species of the Konza Prairie to changing forcings and earlier growing season onset. Understanding these ecosystem conditions furthers the characterization of how driving mechanisms and responses govern semiarid grasslands, and provides an assessment of possible effects on vegetation and habitat to changing climate.

4.1 Site

This study simulates the precipitation dynamics of the Konza Prairie mesic grassland in the Central Great Plains of the United States (40° N, 99.5° W). Precipitation timing (λ: events day^{-1}) and magnitude ($\frac{1}{\alpha}$: depth event^{-1}), along with seasonal potential evaporation, drive the ecology and hydrology of this region (Petrie and Brunsell, 2010). Low annual rainfall (84 cm year^{-1} at Konza; 70 cm year^{-1} for the larger region) promotes dry-mesic grasslands of C_4 grasses and C_3 grass and forb species (Fay et al., 2000). Plant diversity is perhaps maintained by seasonal moisture dynamics and microclimate niches (Harpole and Tilman, 2006; Nippert and Knapp, 2007). Annual Net Primary Production (ANPP) in the Konza prairie is dominated by relatively few, abundant species while spatially-small microclimates have higher species diversity (Knapp et al., 1998). Soils in the region tend to have mollic properties that vary with topography and composition, often with active depths of 1 m or more.

The Central Plains have experienced greater overall climate change than is expected for contemporary climate change (Woodhouse and Overpeck, 1998), but the

rapid onset and direction of current projections may still have disruptive effects (Brunsell et al., 2010). Variation in precipitation, for example, could disrupt vegetation interactions and soil stability, especially in regions with similar historical problems (Fay et al., 2008; Rosenberg et al., 1999). More intensive irrigation requirements may be realized for affected regions, hastening depletion of the Ogallala Aquifer and reducing agricultural productivity (Rosenberg et al., 1999). Land class compositions may also be affected; drier conditions could limit current woody vegetation encroachment, which increased by 154% from 1939-1985 at Konza (Briggs et al., 2005). Increased ambient CO_2 concentration may be another driving factor, but is not included in this analysis because, although dominant species respond to elevated CO_2, the effects are difficult to generalize and are highly species-specific (Morgan et al., 2004). Despite these unknowns, developing analyses of climate effects on grasslands is an important step for understanding and managing these ecosystems.

4.2 Methods

To assess the effects of climate change on mesic grasslands in the Central Plains, we focus on identifying the individual and aggregate effects of less frequent precipitation event timing (λ) and higher magnitude ($\frac{1}{\alpha}$), increased potential evaporation (E_p), and earlier growing season onset on soil moisture (θ), soil evaporation (Es), and transpiration (Tr). We also explore the effect of seasonality in water-use efficiency on carbon assimilation (A) and higher frequency of water-stress events, applying this framework to assess potential effects to Konza Prairie vegetation.

4.2.1 Precipitation simulation

Precipitation was used to force the model using a Poisson process of event timing and magnitude, with daily Monte Carlo generation of precipitation (D'Odorico et al., 2000). Timing and magnitude values for Central Plains grasslands were calculated in the same manner as Petrie and Brunsell (2010), using United States Historical Climatology Network (USHCN) daily precipitation data averages from stations within 1.5° latitude and longitude from the Konza prairie (Williams Jr et al., 2006) [*http* : *//cdiac.ornl .gov/epubs/ndp/ushcn/usa.html*]. Simulations of 500 years at the daily timestep were implemented in the model to output values of soil evaporation, transpiration, carbon assimilation, and soil moisture (Figure 4.1). Variable values for control simulations and for common climate change scenarios are shown in Table 4.1. Additional model parameterizations are shown in Table 4.1.

Precipitation was iterated over timing (λ) and magnitude ($\frac{1}{\alpha}$) with negligible change to mean annual values. Calculated Konza $\lambda = 0.225$ and $\alpha = 1.05$ in simulation 'A' were varied by 4.5 and 4.1% ($\lambda = 0.215$; $\alpha = 1.01$) for the 'B' simulation, by 9 and 8.25% ($\lambda = 0.205$; $\alpha = 0.966$) for the 'C' simulation and 18 and 16% ($\lambda = 0.185$; $\alpha = 0.877$) for the 'D' simulation. These simulations produced mean annual precipitation of 70.0 cm, 69.6 cm, 70.2 cm, and 70.2 cm, respectively, with varying yearly totals. The relationship between λ and α accounts for their varied relation across soil moisture values, as discussed in Petrie and Brunsell (2010).

4.2.2 Water and carbon flux simulation

Surface fraction of soil and vegetation varies across the year. Vegetation fraction (fv) increases for 30 days at the start of the growing season, is maximized during summer, and is depleted for 20 days up to senescence, where it falls to zero until

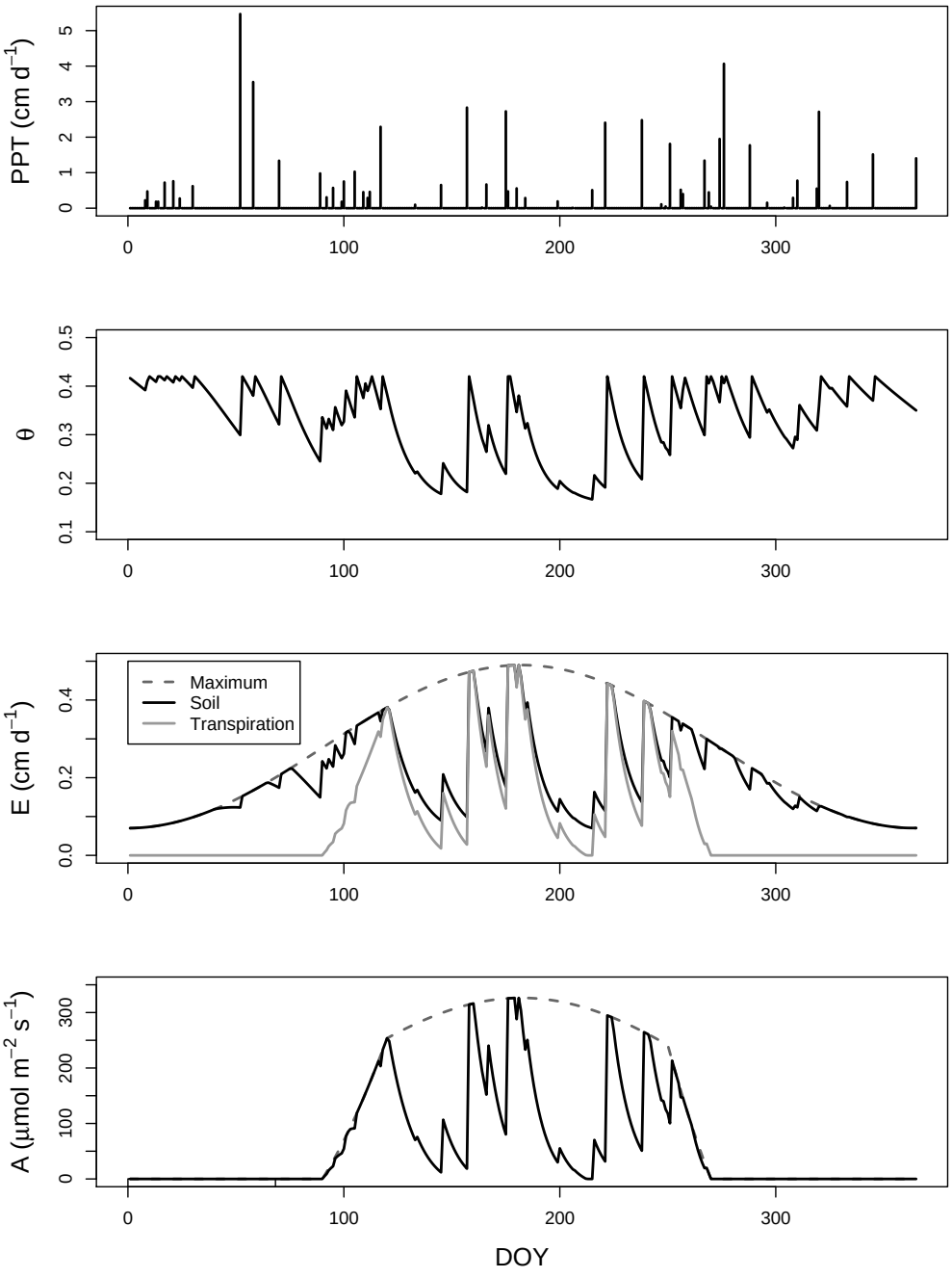

Figure 4.1 One year of modeled precipitation (top) and resulting volumetric soil moisture, water, and carbon fluxes (bottom). Water fluxes are partitioned between transpiration and soil evaporation.

Table 4.1 *Model parameterizations*

Name	Parameter	Value	Units
soil matrix potential	ψ	-.00034	MPa
n/a	b	4.05	n/a
n/a	c	11.1	n/a
hydraulic conductivity	K_s	175	cm d^{-1}
soil porosity	n	0.4	n/a
n/a	β	12.1	n/a
hygroscopic point	θ_h	0.12	m^3 m^{-3}
reduction point	θ^*	0.37	m^3 m^{-3}
field capacity	θ_{fc}	0.42	m^3 m^{-3}
wilting point	θ_w	0.17	m^3 m^{-3}
soil evaporation at θ_w	S_w	0.08	cm d^{-1}
soil active depth	Zr	100	cm
n/a	δ_{et}	0.75	n/a
n/a	ψ_{et}	2.62	d^{-1}
n/a	ω_{et}	0.02	n/a
Control event timing	λ	0.225	events d^{-1}
Scenario event timing	λ	0.185	events d^{-1}
Control event magnitude	$\frac{1}{\alpha}$	0.95	cm $event^{-1}$
Scenario event magnitude	$\frac{1}{\alpha}$	1.14	cm $event^{-1}$
Control mean evapotranspiration	E_{p0}	0.280	cm d^{-1}
Scenario mean evapotranspiration	E_{p0}	0.308	cm d^{-1}
Control growing season onset	n/a	90	Julian Day
Scenario growing season onset	n/a	75	Julian Day
Early and late peak mean WUE	WUE_0	0.12	Julian Day
Early and late peak curve amplitude	δ_{WUE}	0.13	Julian Day
Early and late peak sinusoid frequency	ω_{WUE}	0.03	Julian Day
Early peak phase shift	ψ_{WUE}	5.0	d^{-1}
Late peak phase shift	ψ_{WUE}	2.3	d^{-1}

the following growing season begins. Water stress, defined as soil moisture below the theoretical wilting point ($\theta \leq \theta_w$), for a parameterized resilience period, forces senescence in vegetation for the remainder of the growing season, negating vegetation fraction and fluxes in the model. Analysis focuses on the frequency of these events and their average effect on growing season length. Resilience values are 10 days for all simulations except for Konza vegetation, which is 15 days. Daily maximum carbon assimilation (A_p) is calculated as:

$$A_p = E_p \cdot WUE \tag{4.1}$$

where daily E_p (cm d^{-1}) is calculated from Milly (1994) and water-use efficiency is parameterized by simulation and vegetation. Maximum assimilation has induced seasonality at the beginning and end of the growing season of 30 days from growing season start to maturation and 20 days decline leading to senescence. Transpiration is calculated from carbon assimilation as:

$$Tr = A \cdot \frac{1}{WUE} \tag{4.2}$$

where A is carbon assimilation (μmol m^{-2} s^{-1}) calculated in a piecewise manner (Daly and Porporato, 2005). Soil evaporation is decoupled from transpiration and is calculated in a piecewise manner from Daly and Porporato (2005) as:

$$\begin{aligned} if \quad & 0 < \theta \leq \theta_h; \quad Es = 0 \\ if \quad & \theta_h < \theta \leq \theta_w; \quad Es = S_w \cdot ((\theta - \theta_h)/(\theta_w - \theta_h)) \\ if \quad & \theta_w < \theta \leq \theta^*; \quad Es = S_w + (E_p - E_w) \cdot ((\theta - \theta_h)/(\theta_w - \theta_h)) \\ if \quad & \theta > \theta^*; \quad Es = E_p \end{aligned} \tag{4.3}$$

where θ is volumetric soil moisture (m^3 m^{-3}), θ_h is the hygroscopic point, θ_w is the wilting point, S_w is soil evaporation at wilting point, and θ^* is the reduction point.

These values are theoretical parameterizations for model simulation of fluxes. Total evaporation (E) is the sum of Es and Tr, weighted by the fractional vegetation curve:

$$E = Es \cdot (1 - fv) + Tr \cdot fv \tag{4.4}$$

where fv is the vegetation fraction.

4.2.3 Water-use efficiency

Water-use efficiency simulations explore how vegetation and environment interact across the growing season (Figure 4.2). The first is constant (WUE = 0.12) to assess the impacts of changing climate forcings independent of vegetation phenology. The second simulations vary by out-of-phase sine functions, calculated as:

$$WUE = WUE_0 \cdot [1 + \delta_{WUE} \cdot sin(\omega_{WUE} \cdot h_{day} + \phi_{WUE})] \tag{4.5}$$

where WUE_0 is the annual mean WUE, δ_{WUE} is the amplitude about WUE_0, ω_{WUE} is the frequency of the sinusoid [d^{-1}], h_{day} is the hydrologic day, and ϕ_{WUE} is the phase shift. These values are shown in Table 4.1.

Water-use efficiency measurements collected on the Konza Prairie and parameterizations represent complex effects of leaf temperature, phenology and moisture availability on plant photosynthesis. Daily values reflect varying nonlinear sensitivities of vegetation photosynthesis to internal and external forcings and the average of their variation throughout the day. Between early and late-season water-use efficiency curves (Figure 4.2), for example, values represent differing capabilities of vegetation, aggregate effects of driving variables, and daily to seasonal moisture dynamics. We expect water-use efficiency simulations, however, to retain relevance for carbon and water flux dynamics when these uncertainties are addressed as a component of the

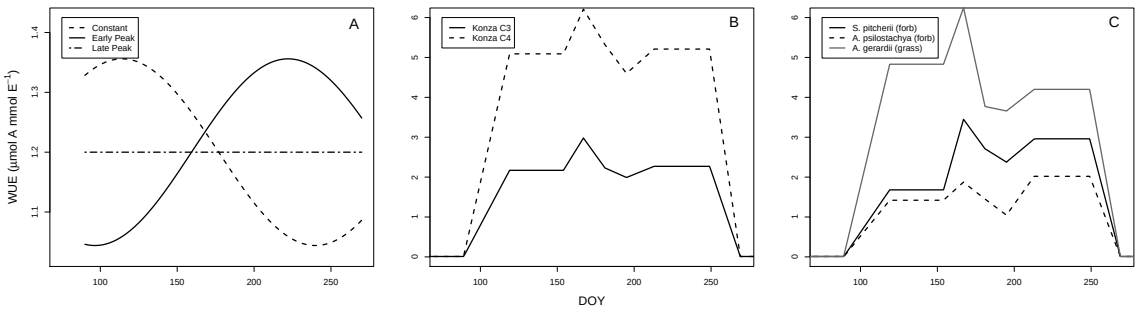

Figure 4.2 Water-use efficiency simulations for (Panel A) constant value and out-of-phase sine curves, (Panel B) Konza C_3 and C_4 vegetation, and (Panel C) *S.pitcherii*, *A.psilostachya*, and *A.gerardii* species (right). Reference growing season onset date is Julian day 90 and date of senescence is Julian day 270. Panels B and C have 30 day maturation periods beginning at start date and 20 day periods of decline leading to senescence.

daily value.

4.2.4 Konza Prairie vegetation

To assess the relationship between vegetation and environment in changing climate, we implement a low-dimensional representation of seasonal water-use efficiency for C_3 and C_4 Konza vegetation and also for one C_4 grass, *Andropogon gerardii*, and two C_3 forbs, *Salvia pitcherii* and *Ambrosia psilostachya*. The focus is to assess whether differences in photosynthetic pathway reflect large-scale vegetation class dynamics or if effects might instead be realized for individual species or habitats. This distinction is important for understanding how climate affects landscape-scale vegetation dynamics and for assessing future grassland compositional responses. The way climate is manifest across space and time will have implications for differing niches of productivity and biodiversity in mesic grasslands.

Carbon assimilation and transpiration measurements for Konza vegetation were taken in-situ during the 2008 growing season on days 155, 168, 182, 196, and 214. Over

this period, 287 instantaneous measurements of photosynthesis (μmol m^{-2} s^{-1}) and transpiration (mmol m^{-2} s^{-1}) were made for C_3 vegetation and 180 for C_4. *S.pitcherii* data includes 24 measurements, 41 for *A.psilostachya*, and 40 for *A.gerardii*. Linear regression techniques were applied with constant values in the early and late periods of the growing season (Figure 4.2).

Water stress events have implications for species' ability to maintain photosynthesis or induce dormancy during periods of limited soil moisture. Research on increased growing season length, seasonal water stress, and vegetation resilience is important for assessing possible changes to composition and species function.

4.3 Results

4.3.1 Changing forcing mechanisms

The effects of increased mean potential evaporation ($\overline{Ep}$), earlier growing season onset, and higher precipitation variation (fewer events of greater magnitude; same annual mean) were analyzed for their effects on water-stress event frequency, and also water and carbon fluxes.

Simulations of climate forcings suggest water stress periods ($\theta \leq \theta_w$) of more than 20 days occur in approximately 2% of years for both C_3 and C_4 species at Konza. For Konza vegetation simulations, we implement a water stress resilience of 15 days, which is expected to maintain full growing season in approximately 90-97% of years.

Individual and aggregate effects of forcings for the constant WUE simulations are shown in Figure 4.3. Panels A and B illustrate growing season reduction from water-stress events for state-space combinations of growing season onset, precipitation simulation, and potential evaporation. Growing season reduction also reflects the frequency of 10-day water-stress events in response to potential evaporation and

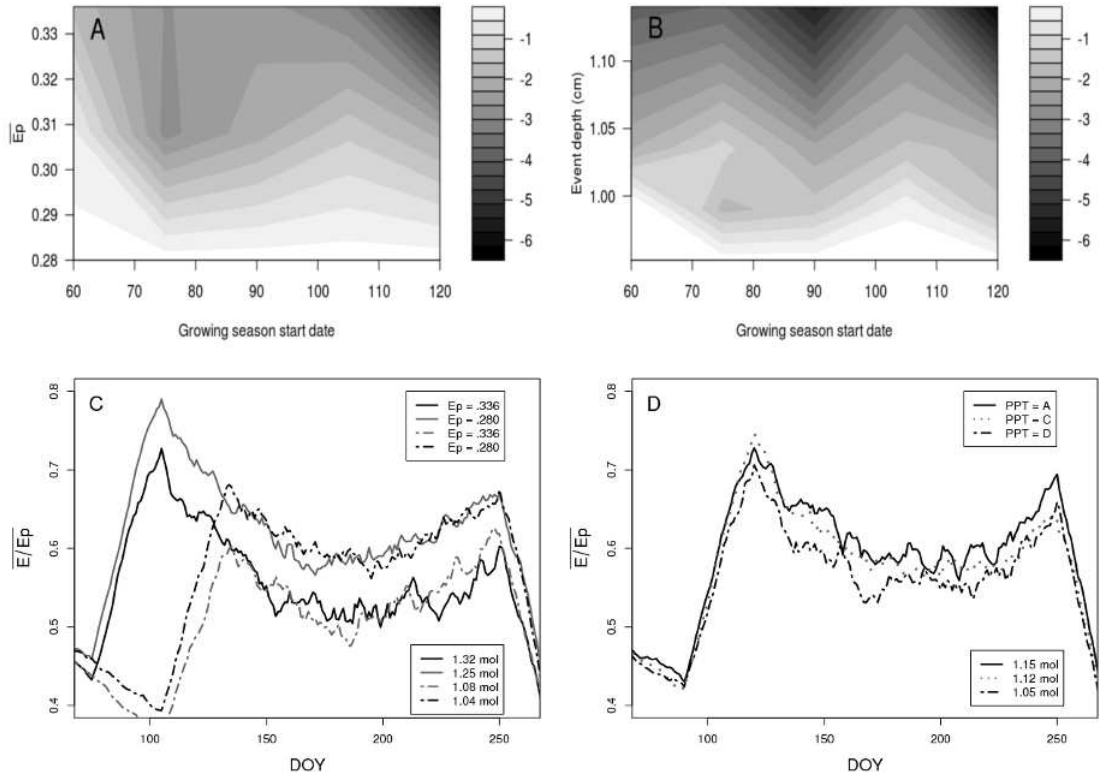

Figure 4.3 (Panel A) Effects of changing potential evaporation and growing season onset on mean growing season length (days); (Panel B) precipitation timing and magnitude (denoted by event depth value) and growing season onset on mean growing season length; (Panel C) potential evaporation and growing season onset on evaporative fraction and total carbon assimilation (mol m^{-2} y^{-1}); (Panel D) precipitation timing and magnitude on total carbon assimilation (mol m^{-2} y^{-1}).

precipitation combinations.

Growing season onset has varied, nonlinear effect throughout the growing season, but shows no discernible effect on water-stress events, suggesting soil moisture is controlled by other factors in summer (Figure 4.3). Earlier onset increases water and carbon fluxes. In panel C, the evaporative fraction $\frac{E}{Ep}$ relationships across mean evaporation values are maintained during summer regardless of growing season start date, with resulting annual carbon assimilation increased by mean evaporation and

growing season. This is important for the seasonal soil moisture dynamics; variation in growing season does not appear to affect summer water fluxes or water-stress events, instead partitioning water fluxes between evaporation and transpiration in the early growing season and elevating early-season carbon fluxes.

Precipitation has important, often limiting effects on soil moisture and resulting fluxes across time (Petrie and Brunsell, 2010). The effects of varying precipitation simulations 'A', 'C', and 'D' are shown in Figure 4.3 panels B and D. Increased precipitation variance simulations promote early-season periods of heightened water and carbon fluxes due to increased soil moisture and sensitivity to event magnitude, with the opposite effect of decreased fluxes and increased water and carbon flux sensitivity to event timing during drier periods. Temporal variance of precipitation has a net negative relationship with carbon assimilation and growing season length on longer timescales (panel D). This is also illustrated by increased probability of water-stress events to precipitation simulations in panel B. Effects of precipitation variance resembles potential evaporation in decreasing soil moisture values, but have conflicting effects on annual mean carbon fluxes (panels C and D).

4.3.2 Early and late-season water-use efficiency

Water-use efficiency defines the vegetative control of modeled carbon assimilation and reflects the interaction of vegetation photosynthesis and limiting environmental conditions. Here, we simplify WUE dynamics as out-of-phase sine curves with early and late peaks (Figure 4.2) to assess how differences in seasonality affect the temporal distribution of fluxes across the growing season, promote differing sensitivities to external forcings, and shape mean annual carbon flux values.

Figure 4.4 illustrates the effect of climate forcing simulations on carbon assimilation between early and late peak water-use efficiency simulations. Values of temporal

variance of assimilation in panels C and D illustrate differences between simulated WUEs and responses to varied precipitation, mean potential evaporation, and growing season onset dates. Differences between WUE simulations for temporal variance of assimilation are most-notable for temporal periods during the growing season; early peak simulations have less difference between maximum and minimum WUE in spring and summer and higher temporal variance of assimilation in spring (panel C), but late peak simulations suggest a greater potential for maximizing increased summer mean evaporation, illustrated by high temporal variance of assimilation in panel D.

Differences between early and late peak WUE simulations produce differing annual mean carbon assimilation (Figure 4.4). Early peak simulations (panels A and E) show near-linear response to temporal variance of precipitation, potential evaporation, and growing season onset, which suggests WUE interacts with individual forcings in a predictable manner and produces uniform effects across forcing magnitude. Late peak simulations of forcing combinations show less-uniformity in annual mean carbon assimilation between drivers, but assimilate more carbon overall (panels B and F). This illustrates seasonal environment and vegetation interaction; early peak simulations incur less-variation in A during the spring (not soil moisture limited) and during the summer (limited by WUE), while late peaks have less-uniform response and higher carbon assimilation due to summer correlation between potential evaporation and WUE peak conditions. This illustrates contrasting environments of high soil moisture versus high potential evaporation with similar correlation to carbon assimilation. All climate forcings heighten the impacts of seasonal WUE differences. How this seasonality is matched by forcing combinations and vegetation phenology in carbon fluxes at daily, seasonal, and annual timescales is a varied and important result of these interactions.

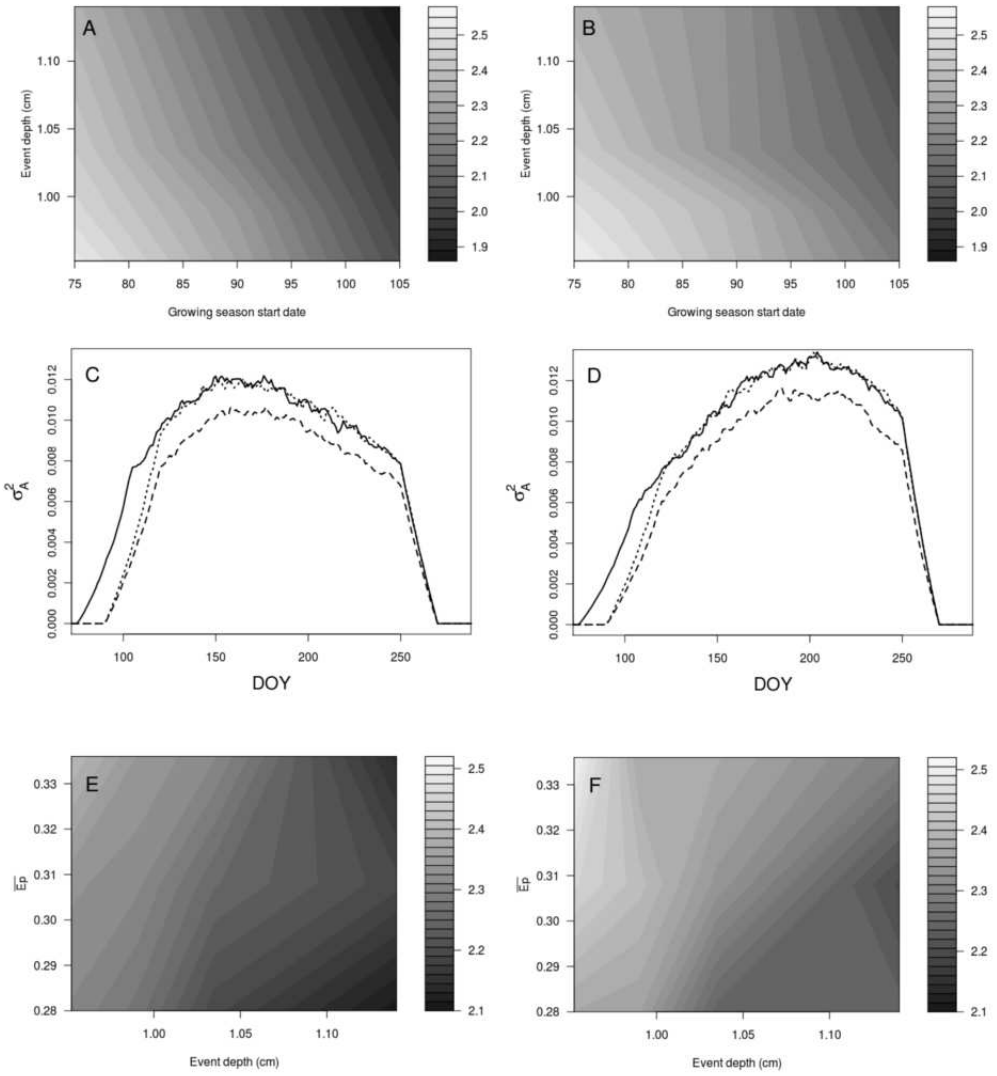

Figure 4.4 (Panel A) Effects of changing precipitation timing and magnitude (denoted by event depth value) and growing season onset on carbon assimilation (mol m^{-2} y^{-1}) for early-peak water-use efficiency simulations; (Panel B) precipitation timing and magnitude and growing season onset on carbon assimilation for late-peak simulations; (Panel C) precipitation timing and magnitude on the temporal variance of carbon assimilation (mol m^{-2} s^{-1}) for early-peak simulations; (Panel D) precipitation timing and magnitude on the temporal variance of carbon assimilation for late-peak simulations; (Panel E) precipitation timing and magnitude and mean evaporation on carbon assimilation (mol m^{-2} y^{-1}) for early-peak water-use efficiency simulations; and (Panel F) precipitation timing and magnitude and mean evaporation on carbon assimilation for late-peak simulations.

4.3.3 Konza Prairie vegetation

Exploring how environment and vegetation interactions might induce change in grassland communities is the third part of this study. Analysis of WUE effects between C_3 and C_4 vegetation at Konza (Figure 4.5) assesses differences in total growing season carbon assimilation to increased mean evaporation (0.28 cm d^{-1} and 0.31 cm d^{-1}) and simulated precipitation in years of 50 cm, 70 cm, and 90 cm. Simulations induce temporal variability in precipitation between years, even where total annual precipitation is comparable. C_3 and C_4 assimilation is reduced comparably in these simulations; by 3%, 8%, and 11% in the low potential evaporation simulations, and 5%, 7%, and 9% in the high potential evaporation simulations. Similarity is likely a product of the similar WUE patterns between C_3 and C_4 at Konza (Figure 4.2), and suggests that WUE maximum, minimum, and early vs. late season differences can correlate and create important temporal periods of carbon assimilation.

These observations provide insight into the annual assimilation differences between C_3 and C_4 classes at Konza (Figure 4.5). Years with lower than average precipitation have greater impact on C_4 carbon assimilation due to the magnitude of C_4 WUE maximum and minimum, which produces a more-elastic negative response to decreased moisture availability (panel B). It follows that C_4 vegetation should have the opposite response for years with higher than average precipitation, but this is not realized (panel B); the carbon assimilation response is perhaps muted by increased precipitation variability. C_3 vegetation has more-moderate responses (Figure 4.5, panel A) because it has a more-uniform WUE curve (Figure 4.2). Statistical precipitation generation complicates this relationship at short timescales and (with the additional impact of potential evaporation) has poor correlation between annual mean precipitation and carbon assimilation (r^2 values of 0.14 and 0.10 for control and climate change simulations, compared to 0.28 and 0.24 for C_3). Further exploration of this is

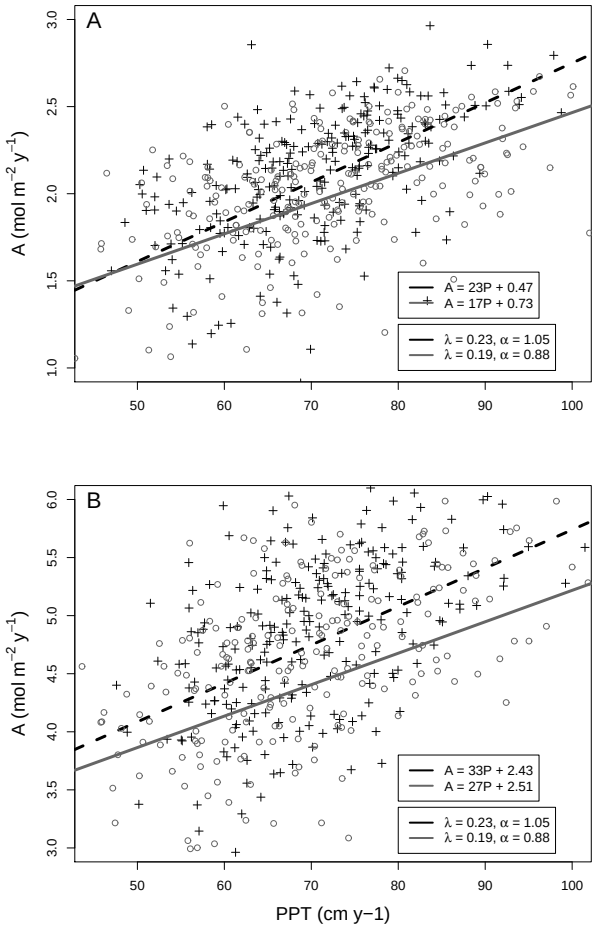

Figure 4.5 (Panel A) Annual carbon assimilation vs. annual precipitation for Konza C_3 and (Panel B) C_4 species. Simulations are varied between potential evaporation (0.28 and 0.31 cm d^{-1}) and precipitation timing (λ) and magnitude ($\frac{1}{\alpha}$).

applied at the species-level for Konza.

How carbon assimilation is affected by C_3 and C_4 species' WUE patterns is an important unknown. Changes in ecosystem functioning could result from shifts in climate or from small shifts in critical habitat and species. We address percent change in annual carbon assimilation to assess how climate and growing season forcings have species-specific effects. Simulations for Two C_3 forb (*S.pitcherii* and *A.psilostachya*) and one C_4 grass (*A.gerardii*) species at Konza under control ($\overline{Ep} = 0.28$, precipitation scenario 'A', start date = 90), climate change ($\overline{Ep} = 0.31$, precipitation scenario 'D', start date = 90), and early start ($\overline{Ep} = 0.31$, precipitation scenario 'D', start date = 75) are assessed (Figure 4.6). Corresponding water-use efficiencies are shown in Figure 4.2, panel C.

S.pitcherii (Figure 4.6, panels A and B) shows differing responses to each forcing scenario. Values of annual carbon assimilation decrease by 10% for years with 50 cm of total precipitation, 4% for years with 70 cm, and 0% for years with 90 cm (panel A), suggesting *S.pitcherii* is susceptible to years of low precipitation but partitions carbon assimilation favorably in years with higher than average amounts. Earlier onset simulations in panel B further this observation; carbon assimilation is decreased by 5% in years with 50 cm but is increased by an average of 2 and 7% in 70 cm and 90 cm years, respectively. Calculated r^2 values for total precipitation and annual carbon assimilation increase from 0.23 for both simulations in panel A to 0.29 for panel B. Although total precipitation is not expected to have a strong correlation to annual carbon assimilation, earlier growing season onset strengthens the impact of total precipitation on carbon flux dynamics for *S.pitcherii*.

A.psilostachya annual carbon assimilation values decrease and increase in a similar manner for climate change and earlier onset simulations in panels C and D. Flux responses are moderated by WUE for *A.psilostachya*, which has low variance

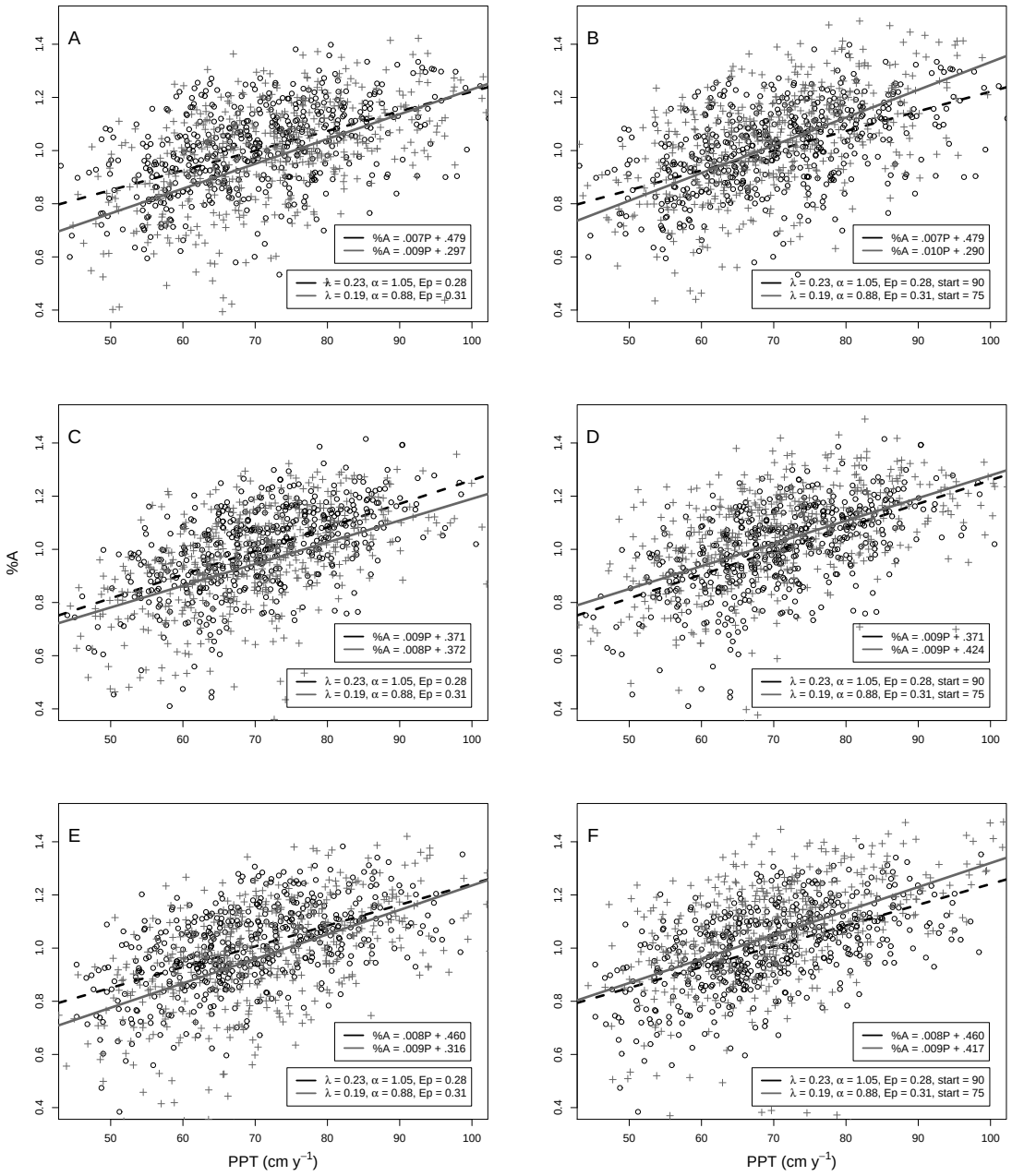

Figure 4.6 Annual carbon assimilation divided by average annual carbon assimilation (mol m^{-2} y$-$1) vs. total annual precipitation (cm y^{-1}) for (Panel A) control and climate change simulations for *S.pitcherii* and with earlier growing season onset (Panel B); (Panel C) control and climate change simulations for *A.psilostachya* and with earlier growing season onset (Panel D); (Panel E) control and climate change simulations for *A.gerardii* and with earlier growing season onset (Panel F). Trendlines for each simulation are shown, where P is annual precipitation and A is annual carbon assimilation.

throughout the year. Instead, annual carbon assimilation reflects external forcings in a similar manner to constant WUE simulations in Figure 4.3. The r^2 value is reduced from 0.33 to 0.18 in panel C, suggesting a different partitioning of sensitivity to forcings with little effect on annual carbon assimilation. In comparison to *S.pitcherii*, *A.psilostachya* is less-responsive to variable external forcings; climate change scenarios present a timing issue between environmental conditions and vegetative controls in shaping flux dynamics.

A.gerardii annual carbon assimilation values decrease across precipitation simulations, increase for earlier growing season simulations, and maintain the same slope for both climate change simulations (panels E and F). *A.gerardii* has the highest variance in annual WUE (Figure 4.2) and assimilates a greater portion of its annual carbon assimilation in the early growing season. Increased precipitation variance, therefore, reduces the probability that periods of high WUE will be maximized. This is illustrated in panel F; *A.gerardii*, like *S.pitcherii*, does not benefit from earlier growing season onset in years with 50 cm of precipitation.

4.4 Discussion

This study presents a number of frameworks to explore climate change impacts. The focus is characterizing the aggregate effects of forcing variation, assessing the role of water-use efficiency in shaping the effects of forcings, and assessing carbon flux responses of C_3 and C_4 vegetation classes and species. Underlying mechanisms, however, have equal importance. These include the temporal interaction of environmental and vegetative controls on carbon assimilation, how increased seasonality might act as a diversifying selector for vegetation species, and relating these to understandings of critical habitat and phenologic periods.

4.4.1 Climate forcing

Environmental conditions throughout the growing season are changed by increased mean evaporation, precipitation variability, and earlier growing season onset. These forcings induce variation in environmental conditions individually and collectively, with varying sensitivity of responses across time. Water and carbon fluxes, for example, are a product of daily sensitivities to forcings scaled to seasonal and annual forcings with differing sensitivities to longer-term environmental trends.

Potential evaporation and precipitation simulations affect soil moisture and carbon assimilation differently (Figure 4.3). Potential evaporation has a positive correlation to water and carbon fluxes, but has a negative correlation to soil moisture. An example is piecewise carbon assimilation determination in the model, where increased potential evaporation increases carbon assimilation at each soil moisture level (greater than the hygroscopic point, $\theta \geq \theta_h$, for example) but decreases soil moisture in the next time step. Precipitation variance affects carbon assimilation through its relationship with daily soil moisture (Petrie and Brunsell, 2010), where limiting soil moisture is most-ameliorated by precipitation event timing, and non-limiting conditions are most-enhanced by event magnitude. Climate change simulations for Konza maintain expected daily and seasonal variable relationships, but forcing changes promote greater daily and inter-seasonal variation.

Earlier growing season lengthens the spring growing period with no apparent effect on summer soil moisture values, illustrated by similar evaporative fraction curves ($\overline{\frac{E}{Ep}}$) in Figure 4.3, panels C and D. This suggests an intermediate condition between the temperate eastern and arid western U.S. of Richardson et al. (2009) and Monson et al. (2005) in annual average fluxes. While water fluxes maintain similar structure in response to earlier onset, carbon assimilation dynamics experience shifts in seasonal partitioning and reduced long term mean values (Figure 4.3). It is important to assess

how these temporal scales relate and are represented by average values.

Some conclusions can be made about how forcings will shape environmental conditions in the Konza Prairie. Flux seasonality is expected to be more-pronounced between the early and late-growing season as the timing of precipitation events decreases water fluxes and potential evaporation increases them. These forcings, in addition to possible earlier growing season onset, will change the seasonal properties of vegetation carbon assimilation, increasing spring carbon assimilation due to earlier onset and reducing it in summer and fall due to the combined effects of potential evaporation and precipitation. Konza grasslands can expect greater annual carbon assimilation at the price of more inter-annual variability, greater seasonality in flux dynamics between periods of limiting and non-limiting soil moisture, and greater variance in daily soil moisture, if not water fluxes, during these seasons. Forcings are not the only factor shaping the effects of climate change, however. Vegetation response to seasonal environment is an important unknown for ecologic functioning. How climate change could affect the gas exchange dynamics of individual species is the subject of the remainder of this discussion.

4.4.2 Water-use efficiency scaling

Water-use efficiency is used in this paper to represent how vegetation photosynthesis responds to environmental conditions. Photosynthesis and related water and carbon fluxes are shaped by three variables in the model: potential evaporation, soil moisture, and water-use efficiency. In the model, daily carbon assimilation is maximized when the most-limiting forcing is maximized; by phenology during maturation in the early growing season, by potential evaporation in the spring, by soil moisture in the summer and fall, and by WUE where other variables are not limiting. Longer temporal periods appear to be of greater importance in determining carbon assimilation dy-

namics and may deviate in response to forcing mechanisms (D'Odorico et al., 2000). The effects of forcing mechanisms at longer timescales are a complex aggregation of potential evaporation, WUE, and precipitation λ and α in creating likely temporal "blocks" of carbon assimilation. Daily carbon assimilation is likely maximized after precipitation events during summer months (high E_p and WUE), while blocks of greatest carbon assimilation are likely during periods where neither soil moisture, potential evaporation, and WUE are limiting, such as late-spring. Peak summer periods for potential assimilation often produce periods of high assimilation, but their occurrence is dependent on precipitation timing; positive and negative effects are not maintained for the same temporal periods across growing seasons.

Early and late-season water-use efficiency simulations illustrate how vegetation and environment compete to shape the dynamics of carbon assimilation. Sensitivity of carbon assimilation to potential evaporation, WUE, and precipitation timing and magnitude depends on seasonal soil moisture values versus seasonal maximum assimilation variation. This maximizes carbon assimilation in late spring under control conditions, but could reduce A as climate change increases growing season seasonality. Changes would disrupt interaction of vegetation versus environment across the growing season. Figure 4.4 late-peak WUE simulations (panels B and F) and linear change for early-peak simulations (panels A and E) suggests forcings are translated differently by these simulations; late-peak simulations show less-linear response in mean annual carbon assimilation but assimilate more carbon overall. While vegetation and environment interactions are not expected to have extreme effects on growing season dynamics, their interaction will reshape small-scale functioning within temporal periods and alter species carbon assimilation partitioning.

4.4.3 Konza vegetation and climate change

Simulations of C_3 and C_4 vegetation illustrate responses of carbon assimilation to forcing and water-use efficiency (Figure 4.5). Both vegetation types have similar responses to these interactions, with C_4 vegetation having greater variation between WUE maximum and minimum (Figure 4.2). How WUE variation corresponds to periods of soil moisture availability and potential evaporation is important; dry growing seasons appear to reduce benefits from early-season WUE peak, and low WUE in the late-season decreases the benefit of years with higher than average precipitation (Figure 4.5). While these dynamics exist presently at Konza, their temporal interaction will be changed by increased forcing variance and species sensitivities (Fay et al., 2000; Collins et al., 2002). Increasing seasonality would benefit vegetation suited to minimize the effects of water stress, vegetation that can maximize favorable conditions or niches, vegetation with specialized phenologic cycles, or vegetation that is less affected by environmental perturbations during the growing season. It does not appear that climate change will favor the C_3 or C_4 photosynthetic pathway; vegetation within these classifications is heterogeneous and will respond to other factors and trends (Collins et al., 2002).

Species-specific simulations suggest that climate change will affect species and niche stability more than it will large-scale vegetation classes or land cover type. This is illustrated by *S.pitcherii*, *A.psilostachya*, and *A.gerardii* in the climate change scenarios. Responses suggest vegetation is affected by the combined impacts of phenology and environment instead of dominant forcings; the same forcings are shaped differently by vegetation WUE (Figure 4.6). Percent increase in carbon assimilation for earlier growing season onset illustrates the differing sensitivities of vegetation to temporal growth periods, temporal carbon partitioning, and effects for mean annual carbon assimilation. *A.psilostachya* is resistant to negative and positive effects

of changing climate possibly from its late-season WUE maximization and low difference between maximum and minimum values, while the seasonality of WUE for *S.pitcherii* (high reliance on late-season assimilation) shows elastic response to precipitation amount and seasonality (Figure 4.6). Increased carbon assimilation in earlier growing season onset simulations may offset carbon assimilation reduction from precipitation and potential evaporation (panels B, D, and F), but also change carbon assimilation partitioning. This partitioning is species-specific and relates to habitat and microclimate; species fitness may have important phenologic periods for growth and reproduction that are not suited increased variability (Fay et al., 2000).

Nonlinear sensitivity of carbon assimilation to forcings creates patterns to assimilation that reflect positive and negative responses during critical periods of the growing season that are specific to each species and, because vegetation at Konza exists in specialized niches, could reflect effects to critical habitat. How these niches exhibit or inhibit the positive and negative effects of increased seasonality during the growing season is unknown. Future impacts are not likely to be driven by a single variable or produce a single result; nonlinearity across forcings and variables, temporal scales, and vegetation responses to environment produce dynamics that resemble current conditions, but with increased intensity of seasonal dynamics and variation between them. How this affects ecological functioning will be a product of forcing combinations across time and the individualized responses of vegetation and habitats to changing dynamics. Growing season change will be more variable than is simulated for the Konza prairie (Julien and Sobrino, 2009), but will have similar effects as climate and vegetation intensify beneficial and deleterious extremes in the growing season.

4.5 Conclusion

Climate change will affect mesic grassland functioning through intensification and diversification of the growing season. While ecosystem responses are difficult to assess, effects to hydrology are more-determinable and depend largely on how climate forcings aggregate to alter soil moisture conditions. Projections for increased potential evaporation and more-variable precipitation are projected to reduce mean daily soil moisture and increase water fluxes. How climate change affects the flux dynamics of grasslands is likely to be a result of the interactions and sensitivity to climate forcings by individual species and these species' ecological interactions throughout the growing season.

Chapter 5

Conclusion

This thesis explores the nonlinear variable interactions and temporal flux dynamics of grassland ecosystems to answer the question of how climate forcings and ecosystem variables interact to shape seasonal water and carbon dynamics. Results illustrate varied temporal sensitivity of water and carbon fluxes to climate forcings, especially precipitation timing and magnitude and potential evaporation. These interactions shape long-term moisture dynamics in the Kansas River basin. Species-specific simulations suggest short-timescales (days to weeks) are more illustrative of vegetation carbon assimilation dynamics and may upscale to reflect annual values. Climate change impacts are not likely to be uniform across space or affect classes of vegetation (such as C_3 and C_4), but will instead increase seasonality of water and carbon fluxes between the early and late growing season. This increased seasonality will diversify growing season moisture availability and carbon assimilation, which could both promote and hinder vegetation functioning at the species-level.

The value of this research is the characterization of temporally variable relationships and their connection to water and carbon fluxes in grasslands. It establishes the ecosystem sensitivity to precipitation timing and magnitude and quantifies the effects

in terms of mass and energy fluxes. Results illustrate unique moisture dynamics in grasslands across the Kansas River Basin precipitation gradient, offering a focused perspective on how precipitation and potential evaporation shape the growing season. This framework is also applied to vegetation water-use efficiency and the interaction of vegetation and forcings in shaping water and carbon flux dynamics. Finally, this research projects the outcomes of regional climate change on vegetation at the Konza Prairie, quantifying the effects future climate could have on grassland species functioning. These projections are important for assessing future ecologic functioning and economic uses of semiarid grasslands, and may be used to anticipate negative scenarios, such as heightened soil erosion or loss of biodiversity, before they develop.

Extensions of this research into microclimates, nutrient availability, and agricultural feasibility assessments would be beneficial for understanding how climate change will shape semiarid and other water-limited regions. Topography alters the soil depth and water availability of microclimates within grassland ecosystems, and might act to enhance or diminish the effects of seasonal fluctuations. Seasonal nutrient availability could represent critical phenologic periods in the model to analyze how altered soil moisture inhibits or favors vegetation growth and reproduction strategies. Assessing future agricultural moisture requirements would require a relatively easy set of parameterizations to quantify water fluxes from crops. A good step, before all of the above, is to first validate the model against eddy covariance data for mass and energy fluxes to address whether or not it is robust for more-empirical applications beyond characterization of variable nonlinearities. Validation is perhaps most important and will dictate future model uses and perhaps resemble the overall capabilities of low-dimensional analysis techniques.

A more-directed look at the driving relationships and feedbacks that create and interconnect ecosystems helps to better describe the uniqueness of landscape hetero-

geneity, in general, and grasslands, specifically. Semiarid ecosystems are shaped by subtle processes over long timescales, but have interesting, complex dynamics across varied landscapes and environmental conditions. The illustrative quality of semiarid ecosystems is how this subtlety of interactions creates the functioning landscape. As the value of semiarid ecosystems unfolds and gains weight in the sciences, I hope that regions including the Konza Prairie are incorporated more in the ideal of natural places and wilderness not as a pedestal of metaphysics, but as an active, dynamic illustration of the potential human and ecological advantage of interaction with the natural world.

Bibliography

Alessandri, A., Navarra, A., 2008. On the coupling between vegetation and rainfall inter-annual anomalies: Possible contributions to seasonal rainfall predictability over land areas. Geophysical Research Letters 35 (2).

Angert, A., Biraud, S., Bonfils, C., Henning, C., Buermann, W., Pinzon, J., Tucker, C., Fung, I., 2005. Drier summers cancel out the co2 uptake enhancement induced by warmer springs. Proceedings of the National Academy of Sciences 102 no. 31, 10823–10827.

Betts, R., Cox, P., Lee, S., Woodward, F., 1997. Contrasting physiological and structural vegetation feedbacks in climate change simulations. Nature 387, 796–799.

Bormann, H., Diekkruger, B., 2003. Possibilities and limitations of regional hydrological models applied within an environmental change study in Benin (West Africa). Physics and Chemistry Of the Earth 28 (33-36), 1323–1332.

Briggs, J., Knapp, A., Blair, J., Heisler, J., Hoch, G., Lett, M., McCarron, J., 2005. An ecosystem in transition: causes and consequences of the conversion of mesic grassland to shrubland. Bioscience 55, 243–254.

Brunsell, N., 2006. Characterization of land-surface precipitation feedback regimes with remote sensing. Remote Sensing of Environment 100 (2), 200–211.

Brunsell, N., Buck, T., Ham, J., Billings, S., Nippert, J., 2009. Surface-atmosphere coupling of carbon and water flux in a mixed grassland. In review.

Brunsell, N., Gillies, R., 2003. Length scale analysis of surface energy fluxes derived from remote sensing. Journal of Hydrometerology 4, 1212–1219.

Brunsell, N., Gillies, R., 2003. Scale issues in land-atmosphere interactions: implications for remote sensing of the surface energy balance. Agricultural and Forest Meterology 117 (3-4), 203–221.

Brunsell, N., Jones, A., Jackson, T., Feddema, J., 2010. Seasonal trends in air temperature and precipitation in ipcc ar4 gcm output for kansas, usa: evaluation and implications. International Journal of Climatology doi:10.1002/joc.1958, in press.

Brunsell, N., Young, C., 2008. Land surface response to precipitation events using MODIS and NEXRAD data. International Journal of Remote Sensing 29 (7), 1965–1982.

Budyko, M., 1974. Climate and Life. Academic Press.

Caylor, K., Rodriguez-Iturbe, I., 2003. Soil moisture and plant stress dynamics along the kalahari precipitation gradient. Journal of Geophysical Research 108 no. D3, 1–8.

Claussen, M., Brovkin, V., Ganapolski, A., 2001. Biogeophysical versus biogeochemical feedbacks of large-scale land cover change. Geophysical Research Letters 28 no. 6, 1011–1014.

Collins, S., Glenn, S., Briggs, J., 2002. Effect of local and regional processes on plant species richness in tallgrass prairie. Oikos 99, 571–579.

Daly, E., Porporato, A., 2005. A review of soil moisture dynamics: From rainfall infiltration to ecosystem response. Environmental Engineering Science 22 (1), 9–24.

Daly, E., Porporato, A., 2006. Impact of hydroclimatic fluctuations on the soil water balance. Water Resources Research 42, 1–11.

D'Odorico, P., Ridolfi, L., Porporato, A., Rodriguez-Iturbe, I., 2000. Preferential states of seasonal soil moisture: The impact of climate fluctuations. Water Resources Research 36 (8), 2209–2219.

Eagleson, P., 1982. Ecological Optimality in Water-limited Natural Soil-vegetation Systems .1. Theory and Hypothesis. Water Resources Research 18 (2), 325–340.

Emmerich, W., 2007. Ecosystem water use efficiency in a semiarid shrubland and grassland community. Rangeland Ecology & Management 60, 464–470.

Epstein, H., Laurenloth, W., Burke, I., Coffin, D., 1996. Ecological responses of dominant grasses along two climactic gradients in the great plains of the united states. Journal of Vegetation Science 7, 777–788.

Fay, P., Carlisle, J., Knapp, A., Blair, J., Collins, S., 2000. Altering rainfall timing and quantity in a mesic grassland ecosystem: design and performance of rainfall manipulation shelters. Ecosystems 3, 308–319.

Fay, P. A., Kaufman, D. M., Nippert, J. B., Carlisle, J. D., Harper, C. W., 2008. Changes in grassland ecosystem function due to extreme rainfall events: implications for responses to climate change. Global Change Biology 14 (7), 1600–1608.

Guswa, A., Celia, M., Rodriguez-Iturbe, I., 2002. Models of soil moisture dynamics in ecohydrology: A comparative study. Water Resources Research 38 (9).

Ham, J., Knapp, A., 1998. Fluxes of co2, water vapor, and energy from a prairie ecosystem during the seasonal transition from carbon sink to carbon source. Agricultural and Forest Meterology 89, 1–4.

Harpole, W., Tilman, D., 2006. Non-neutral patterns of species abundance in grassland communities. Ecology Letters 9, 15–23.

Houghton, J., 2001. The science of global warming. Interdisciplinary Science Reviews 26 no. 4, 247–257.

Ivanov, V. Y., Bras, R. L., Vivoni, E. R., 2008. Vegetation-hydrology dynamics in complex terrain of semiarid areas: 1. A mechanistic approach to modeling dynamic feedbacks. Water Resources Research 44 (3), 10.1029/2006WR005588.

Jacobs, A., Heusinkveld, B., Holtslag, A., 2003. Carbon dioxide and water vapor flux densities over a grassland area in the netherlands. International Journal of Climatology 23, 1663–1675.

Jarvis, P., 1976. The interpretation of the variations in leaf water potential and stomatal conductance found in canopies in the field. Phil. Trans. R. Soc. Lond. 273, 593–610.

Jones, A., Brunsell, N., 2009. Energy balance partitioning and net radiation controls on soil moisture-precipitation feedbacks. Earth Interactions 13.

Julien, Y., Sobrino, J., 2009. Global land surface phenology trends from gimms database. International Journal of Remote Sensing 13, 3495–3513.

Kalma, J. D., McVicar, T. R., McCabe, M. F., 2008. Estimating Land Surface Evaporation: A Review of Methods Using Remotely Sensed Surface Temperature Data. Surveys in Geophysics 29 (4-5), 421–469.

Kleidon, A., Schymanski, S., 2008. Thermodynamics and optimality of the water budget on land: A review. Geophysical Research Letters 35, 1–6.

Knapp, A., Briggs, J., Hartnett, D., Collins, S. (Eds.), 1998. Grassland dynamics: long-term ecological research in tallgrass prairie. Long-Term Ecological Research Network Series.

Koster, R., Suarez, M., 1999. A simple framework for examining the interannual variability of land surface moisture fluxes. Journal of Climate 12 (7), 1911–1917.

Laio, F., Porporato, A., Fernandez-Illescas, C., Rodriguez-Iturbe, I., 2001a. Plants in water-controlled ecosystems: active role in hydrologic processes and response to water stress iv. discussion of real cases. Advances in Water Resources 24, 745–762.

Laio, F., Porporato, A., Ridolfi, L., Rodriguez-Iturbe, I., 2001b. Plants in water-controlled ecosystems: active role in hydrologic processes and response to water stress - ii. probabilistic soil moisture dynamics. Advances in Water Resources 24 (7), 707–723.

Laio, F., Porporato, A., Ridolfi, L., Rodriguez-Iturbe, I., 2002. On the seasonal dynamics of mean soil moisture. Journal of Geophysical Research-Atmospheres 107 (D15), 10.1029/2001JD001252.

Lokke, D., Kidman, R., 1963. Bibliography of kansas meterology: Precipitation. Transactions of the Kansas Academy of Science 66 no. 3, 417–425.

Makela, A., Berninger, F., Hari, P., 1996. Optimal control of gas exchange during drought: Theoretical analysis. Annals of Botany 77 (5), 461–467.

Milly, P., 1994. Climate, soil water storage, and average annual water balance. Water Resources Research 30 no. 7, 2143–2156.

Monson, R., Sackschewsky, M., Williams III, G., 1986. Field measurements of photosynthesis, water-use efficiency, and growth in angropyron smithii (c3) and bouteloua gracilis (c4) in the colorado shortgrass steppe. Oecologia 68, 400–409.

Monson, R., Sparks, J., Rosentiel, T., Scott-Denton, L., Huxman, T., Harley, P., Turnipseed, A., Burns, S., Backlund, B., Hu, J., 2005. Climatic influences on net ecosystem co2 exchange during the transitions from wintertime carbon source to springtime carbon sink in a high-elevation, subalpine forest. Oecologia 146, 130–147.

Morgan, J., Pataki, D., Korner, C., Clark, H., Del Grosso, S., Grunzweig, J., Knapp, A., Mosier, A., Newton, P., Niklaus, P., Nippert, J., Nowak, P., Parton, W., Polley, H., Shaw, M., 2004. Water relations in grassland and desert ecosystems exposed to elevated atmospheric co2. Oecologia 140, 11–25.

Nippert, J., Fay, P., Carlisle, J., Knapp, A., Smith, M., 2009. Ecophysiological responses of two dominant grasses to altered temperature and precipitation regimes. Acta Oecologia 35, 400–408.

Nippert, J., Fay, P., Knapp, A., 2007. Photosynthetic traits in c3 and c4 grassland species in mesocosm and field environments. Environmental and Experimental Botany 60, 412–420.

Nippert, J., Knapp, A., 2007. Soil water partitioning contributes to species coexistence in tallgrass prairie. Oikos 116, 1017–1029.

Niu, S., Yuan, Z., Y, Z., Liu, W., Zhang, L., Huang, J., Wan, S., 2005. Photosynthetic responses of c3 and c4 species to seasonal water variability and competition. Journal of Experimental Botany 56 no. 421, 2867–2876.

Petrie, M., Brunsell, N., 2010. The role of precipitation variability on the ecohydrology of grasslands. Ecohydrology, in review.

Porporato, A., Daly, E., Rodriguez-Iturbe, I., 2004. Soil water balance and ecosystem response to climate change. American Naturalist 164 (5), 625–632.

Porporato, A., Laio, F., Ridolfi, L., Caylor, K., Rodriguez-Iturbe, I., 2003. Soil moisture and plant stress dynamics along the Kalahari precipitation gradient. Journal of Geophysical Research-Atmospheres 108 (D3), 10.1029/2002JD002448.

Porporato, A., Laio, F., Ridolfi, L., Rodriguez-Iturbe, I., 2001. Plants in water-controlled ecosystems: active role in hydrologic processes and response to water stress - III. Vegetation water stress. Advances in Water Resources 24 (7), 725–744.

Raupach, M., 1995. Vegetation atmosphere interaction and surface conductance at leaf, canopy and regional scales. Agricultural and Forest Meterology 73, 151–179.

Richardson, A., Hollinger, D., Dail, D., Lee, J., Munger, J., O'Keefe, J., 2009. Influence of spring phenology on seasonal and annual carbon balance in two contrasting new england forests. Tree Physiology 29, 321–331.

Ridolfi, L., D'Odorico, P., Porporato, A., Rodriguez-Iturbe, I., 2000a. Duration and frequency of water stress in vegetation: An analytical model. Water Resources Research 36 (8), 2297–2307.

Ridolfi, L., D'Odorico, P., Porporato, A., Rodriguez-Iturbe, I., 2000b. Impact of climate variability on the vegetation water stress. Journal of Geophysical Research-Atmospheres 105 (D14), 18013–18025.

Rodriguez-Iturbe, I., Porporato, A., Laio, F., Ridolfi, L., 2001. Plants in water-

controlled ecosystems: active role in hydrologic processes and response to water stress - I. Scope and general outline. Advances in Water Resources 24 (7), 695–705.

Rodriguez-Iturbe, I., Porporato, A., Ridolfi, L., Isham, V., Cox, D., 1999. Probabilistic modelling of water balance at a point: the role of climate, soil and vegetation. Proceedings of the Royal Society A-Mathematical Physical and Engineering Sciences 455 (1990), 3789–3805.

Rosenberg, N., Epstein, D., Wang, D., Vail, L., Srinivasan, R., Arnold, J., 1999. Possible impacts of global warming on the hydrology of the ogallala aquifer region. Climatic Change 42 no. 4, 677–692.

Sridhar, V., Elliott, R., Chen, F., Brotzge, J., 2002. Validation of the noah-osu land surface model using surface flux measurements in oklahoma. Journal of Geophysical Research 107, 1–18.

Stephenson, N., 1998. Actual evapotranspiration and defecit: biologically meaningful correlates of vegetation distribution across spatial scales. Journal of Biogeography 25, 855–870.

Teuling, A., Seneviratne, S., Williams, C., Troch, P., 2006b. Observed timescales of evapotranspiration response to soil moisture. Geophysical Research Letters 33, 1–5.

Teuling, A., Uijlenhoet, R., Hupet, F., Troch, P., 2006. Impact of plant water uptake strategy on soil moisture and evapotranspiration dynamics during drydown. Geophysical Research Letters 33 (3), 10.1029/2005GL025019.

Vermeire, L., Heitschmidt, R., Rinella, M., 2009. Primary productivity and precipitation-use efficiency in mixed-grass prairie: a comparison of northern and southern us sites. Rangeland Ecology & Management 62, 230–239.

Vico, G., Porporato, A., 2008. Modelling c3 and c4 photosynthesis under water-stressed conditions. Plant Soil 313, 187–203.

Williams Jr, C., Vose, R., Easterling, D., Menne, M., 2006. United states historical climatology network daily temperature, precipitation, and snow data. tech. rep. ornl/cdiac-118, ndp-070, carbon dioxide information analysis center, oak ridge national laboratory, oak ridge, tennessee.

Woodhouse, C., Overpeck, J., 1998. 2000 years of drought variability in the central united states. Bulletin of the American Meterological Society 79 no. 12, 2693–2714.